

1-1516

A DEMONSTRATION PROJECT ON  
INSTRUMENTATION OF A  
FLEXIBLE PAVEMENT

FINAL REPORT

OHIO DEPARTMENT OF TRANSPORTATION and  
FEDERAL HIGHWAY ADMINISTRATION

Principal Investigators:

Shad M. Sargand

Glenn A. Hazen

Graduate Research Assistants:

Jason L. McCauley

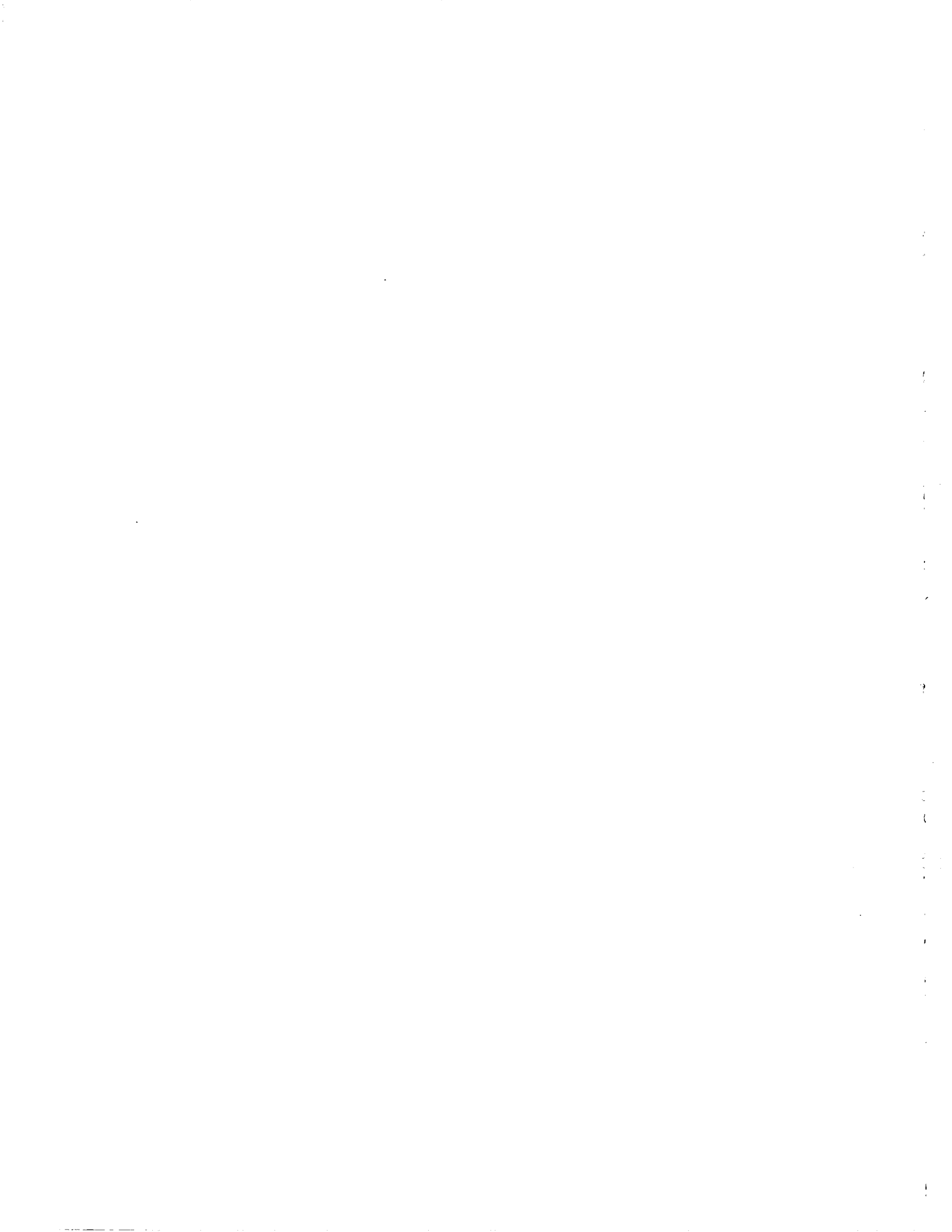
Daniel J. Schweiger

"The contents of this report reflect the views of the authors, who are responsible for the facts and accuracy of the data presented herein. The contents do not necessarily reflect the official views of the Ohio Department of Transportation or the Federal Highway Administration. This report does not constitute a standard, specification or regulation."

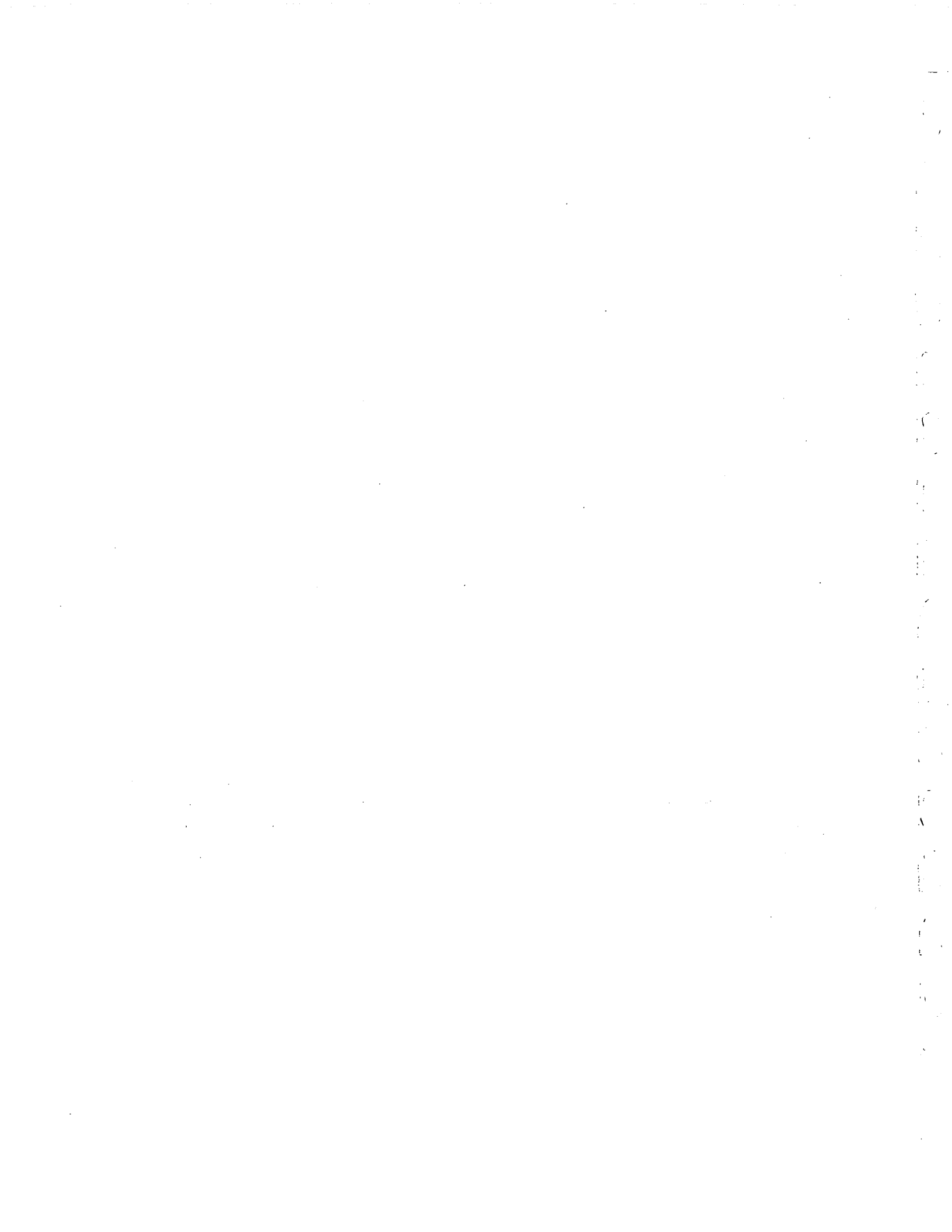
Ohio University  
Center for Geotechnical and Environmental Research  
Civil Engineering Department

April 1997

Roger R.



1. Report No. FHWA/OH-97/002	2. Government Accession No.	3. Recipient's Catalog No.	
4. Title and Subtitle A DEMONSTRATION PROJECT ON INSTRUMENTATION OF A FLEXIBLE PAVEMENT		5. Report Date October, 1996	6. Performing Organization Code
7. Author(s) Shad Sargand, Glenn A. Hazen		8. Performing Organization Report No.	
9. Performing Organization Name and Address Ohio University Department of Civil Engineering Athens, OH 45701		10. Work Unit No. (TRAIS)	
12. Sponsoring Agency Name and Address Ohio Department of Transportation 25 S. Front St. Columbus, OH 43215		11. Contract or Grant No. State Job No. 14516(0)	
15. Supplementary Notes Prepared in cooperation with the U.S. Department of Transportation, Federal Highway Administration		13. Type of Report and Period Covered Final Report	
16. Abstract <p>An instrumentation plan and installation techniques were developed for a full-scale asphalt concrete test pavement. Six asphalt pavement test sections were constructed over an asphalt-treated base, cement-treated base, New Jersey base, Iowa base, 8 inch 304 base and 6 inch 304 base. Upon completion of test sections, moisture, temperature, vertical deflections, pressures, and strains were measured as the pavement was subjected to non-destructive testing. Data were compared to predictions of a finite element model. Field data indicate that the deflection of asphalt with asphalt-treated base varies significantly with change in temperature. Deflection of the pavement over cement-treated base was the lowest. Among the non-treated bases, the bases with the larger aggregate experienced less deflection. The OU-PAVE finite element program predicted with reasonable accuracy maximum deflection and the deflection profile.</p>		14. Sponsoring Agency Code	
17. Key Words pavement, base, asphalt concrete, FEM, strain, deflection, moisture, temperature, instrumentation		18. Distribution Statement No Restrictions. This document is available to the public through the National Technical Information Service, Springfield, Virginia 22161	
19. Security Classif. (of this report) Unclassified	20. Security Classif. (of this page) Unclassified	21. No. of Pages	22. Price



# A DEMONSTRATION PROJECT ON INSTRUMENTATION OF A FLEXIBLE PAVEMENT

## TABLE OF CONTENTS

<u>Title</u>	<u>Page No.</u>	
Chapter 1	Introduction	1
1.1	General Statement and Outline of Research	1
1.2	Literature Review	2
1.3	Objectives	5
Chapter 2	Instrumentation and Installation Procedures	6
2.1	Project Location	6
2.2	Description of the Sections	6
2.3	Instrumentation Selection	9
	2.3.1 Strain Measurement	11
	2.3.2 Deflection Measurement	12
	2.3.3 Moisture Measurement	14
	2.3.4 Temperature Measurement	14
	2.3.5 Interface Pressure Measurements	15
2.4	Instrumentation Layout	16
2.5	Sensor Installation	18
	2.5.1 Soil Moisture Probes	18
	2.5.2 Earth Pressure Cells	18
	2.5.3 Single Point Thermocouples	19
	2.5.4 Single Layer Deflectometers (SLD)	19
	2.5.5 Strain Gauges (Dynatest, HBM)	21
	2.5.6 Instrumentation Cabling and Labeling	21
	2.5.7 Instrumentation Location Reference	23
Chapter 3	Testing Procedures and Data Collection	25
3.1	Testing	25
	3.1.1 FWD Testing Equipment	25
	3.1.2 Testing Procedure	27
3.2	Environmental Data	29
	3.2.1 Testing Equipment	29
	3.2.2 Testing Procedure	30
3.3	Summary of all Sensor Losses	30
	3.3.1 Instrumentation	30
	3.3.2 Traffic Control	32

<u>Title</u>	<u>Page No.</u>
Chapter 4	34
4.1	34
4.2	34
4.2.1	34
4.2.2	35
4.2.3	37
4.2.4	37
4.2.5	39
4.3	39
4.3.1	40
Chapter 5	41
5.1	41
5.2	41
5.3	44
5.3.1	45
5.3.2	58
5.3.3	62
5.4	71
Chapter 6	72
6.1	72
6.2	72
6.2.1	73
6.2.2	73
6.2.3	73
6.3	75
6.4	75
6.5	77
6.6	77
6.7	84
Chapter 7	85
7.1	85
7.2	85
7.2.1	85
7.2.2	85
7.2.3	86
7.3	88
References	89

## LIST OF FIGURES

<u>Figure No.</u>	<u>Title</u>	<u>Page No.</u>
Figure 2.1	Plan and Cross-Sectional Views of a Typical Instrumentation Site	10
Figure 2.2	Single Layer Deflectometer (SLD) Construction	13
Figure 2.3	Typical Instrumentation Location	17
Figure 2.4	Exposed Brass Cap of the Single Level Deflectometer	22
Figure 2.5	Epoxy Used to Fix Single Level Deflectometer Unit	22
Figure 3.1	FWD Data Acquisition Equipment	26
Figure 3.2	FWD Deflection Printout	28
Figure 4.1	Variation of Asphalt Modulus with Temperature	38
Figure 5.1	Comparison of Accelerometer and LVDT Deflection	47
Figure 5.2	SLD Responses from December FWD Test	52
Figure 5.3	SLD Responses from April FWD Test	53
Figure 5.4	Pavement Deflection (SLD) Versus Pavement Temperatures	55
Figure 5.5	Pavement Deflection (Geophone) Versus Pavement Temperature	56
Figure 5.6	Pavement Deflection Versus Section Tested	57
Figure 5.7	Pavement and Base Deformation Versus Section Tested	59
Figure 5.8	Time Response of Pressure Cells Subjected to FWD Loading	60
Figure 5.9	Base Pressures Versus Section	63
Figure 5.10	Subgrade Pressures Versus Section	64
Figure 5.11	HBM Response to FWD Testing	68
Figure 5.12	Dynatest Response to FWD Testing	69
Figure 6.1	ILLI-PAVE Subgrade Material Models for Stiff, Medium Stiff, Soft and Very Soft Soils From [19]	74
Figure 6.2	Comparison of FWD Deflections of Section 3 for April Test	76
Figure 6.3	Comparison of FWD Deflections of Section 1 for September Test	78
Figure 6.4	Comparison of FWD Deflections of Section 3 for September Test	79
Figure 6.5	Comparison of FWD Deflections of Section 5 for September Test	80
Figure 6.6	Comparison of FWD Deflections of Section 1 for January Test	81
Figure 6.7	Comparison of FWD Deflections of Section 3 for January Test	82
Figure 6.8	Comparison of FWD Deflections of Section 5 for January Test	83

## LIST OF TABLES

<u>Table No.</u>	<u>Title</u>	<u>Page No.</u>
Table 2.1	Asphalt Thicknesses, Base Types and Thicknesses	7
Table 2.2	Description of Non-Stabilized Base Materials	8
Table 3.1	A List of Sensors Still Working at Completion of Project	31
<u>Table No.</u>	<u>Title</u>	<u>Page No.</u>
Table 5.1	Environmental Data for Asphalt Concrete	42
Table 5.2	Comparison of Pavement Deflections when Loaded with FWD	46
Table 5.3	Deflections for Single Level Deflectometers from FWD Tests	49
Table 5.4	Pressure Cell Data for FWD Loading	61
Table 5.5	Strain Gauge Response for FWD	65

## CHAPTER 1

### INTRODUCTION

#### 1.1 GENERAL STATEMENT AND OUTLINE OF RESEARCH

Asphalt concrete is used throughout the United States in the construction of roads and major highways. Repair of these pavements cost taxpayers millions of dollars each year. Reduction of repair costs should be achieved with better understanding of pavement performance. Therefore, it is necessary to study structural pavement performance based upon the factors that may influence degradation. Two major factors that influence pavement deterioration are loading conditions and environmental factors. Procedures for design and analysis of flexible pavements are based on accepted empirical methods developed in the field from past experience. Currently, efforts have been directed toward development of new design and analysis procedures employing mechanistic theories.

Of concern to model development based upon mechanistic theories, is that it is difficult, if not impossible, to include all conditions that influence pavement deterioration. Testing helps deal with this concern and provides data on the influence of the environment and realistic loading conditions. New design method verification is benefited by the construction of full-scale instrumentations sites to measure *in-situ* responses.

This research project sought to develop an instrumentation plan and installation techniques for a full-scale asphalt concrete (AC) test pavement. Placement of instrumentation commenced with the paving operation. The first section was instrumented in August 1993, and all sections were

complete by November 1993. Six sections were constructed with different base types, base thicknesses, and pavement thicknesses. After completion of the sections, accurate measurements were made of response of pavement sections subjected to nondestructive testing (NDT). These responses were measured as vertical deflections, pressures, and strains within the pavement. Data were analyzed and compared with respect to base type and thickness, asphalt concrete thickness, base and subgrade moisture content, and temperature gradient.

## 1.2 LITERATURE REVIEW

A limited number of field studies have been conducted and published on flexible pavement. The kind of instrumentation used for measuring deflection, soil moisture, temperature, pore-water pressure, and strain was not consistent in these studies. Not only were the systems used for monitoring responses different, but installation technique also varied with investigator.

Bonaquist, Surdahl, and Mogawer (1) reported on the effects of truck tire pressure on flexible pavement performance. Their pavement instrumentation consisted of thermocouples and moisture cells at various depths in the pavement, strain gauges at the bottom of the asphalt concrete layer, and a Linear Variable Differential Transformer (LVDT) used for measuring surface deflection. An Accelerated Loading Facility testing machine was used to simulate traffic and various combinations of loads and tire pressures. The response evaluation showed that increasing the tire pressure had little effect on surface deflection and strain at the bottom of the asphalt concrete layer. The evaluation also showed that test section rutting and cracking increased with higher tire pressure. In these sections, however, the temperature in the asphalt concrete was much higher.

Sebaaly, Tabatabaee, and Scullion (2) evaluated pavement response under actual truck

loading and Falling Weight Deflectometer (FWD) testing. Three different types of strain gauges were used to measure the longitudinal strain at the bottom of the asphalt concrete layer, including the Dynatest H gauge, the Kyowa H gauge, and instrumented core gauges. A multi-depth deflectometer (MDD) was also used to measure the deflection throughout the depth of the pavement structure. They presented backcalculation techniques in conjunction with strain gauge data, FWD data, and MDD results. The backcalculated moduli of all the pavement layers were significantly affected by the mode of loading (i.e., FWD vs. truck). The modulus of the asphalt concrete was reduced significantly by reducing the speed of the truck. Analysis of strain and MDD data concurred with the backcalculated results, i.e., the speed of the truck had a notable effect on the modulus of the asphalt concrete layer.

Tabatabaee and Sebaaly (3) discussed the various types of strain gauges, pressure cells, deflectometers, and temperature indicators that have been used to instrument flexible pavements. They compared different core gauges to the H-gauges and made recommendations on their use. Single Layer Deflectometers (SLD) and Multi-Depth Deflectometers (MDD) were compared against one another and the pros and cons of each were presented. Suggestions for installation of these assemblies were also made. The problems with calibrating pressure cells were discussed and recommendations on how to overcome these problems were presented.

Brown (4) reported on the use of earth pressure cells in pavement monitoring, as well as installation and calibration and indicated that installed instruments should withstand the rigors of construction, both environmentally and mechanically. Brown noted that in order to reduce error, controlled laboratory calibration is desirable and that calibration should be done under conditions that reproduce the field situation. Suggestions included orienting the pressure cell with the

diaphragm up in a precut recess during installation and taking care that no large soil particle is positioned on the diaphragm when backfilling is complete.

Ulitz and Busch (5) conducted a test on a two-layer road structure. The layers consisted of a bituminous base and a silty sand subgrade. Thermocouples were used to measure temperatures. H-gauges were used to measure the strain throughout the asphalt concrete. Pressure cells were used to measure the soil stresses. Strains in the subgrade were measured by linear variable displacement transducers (LVDTs). Accelerometers or geophones were used to measure the deflections. *In-situ* testing was accomplished by using the FWD and the lightweight deflectometer (LWD). The validity of different design procedures was checked by Road-Testing Machines (RTMs). They concluded that the RTM appeared to be well suited to study various climate conditions and effects of heavy traffic loading on full-scale pavement structures.

Nazarian and Chai (6) studied how layered-elastic theory and non-destructive testing (NDT) devices could be used together to predict the behavior of pavement. Four, two-dimensional geophones were encapsulated in an epoxy-resin mix using 4 inch outside-diameter, polyvinyl chloride (PVC) pipe as a mold. The geophones were placed in a borehole with the NDT loading mechanism placed on top. Deflections from seven NDT devices were used to find the closeness of calculated and measured responses of pavement. The testing showed that theoretical deflections, not affected by load-induced non-linearity, may be close to measured deflections. However, they concluded that theoretical deflections in the body of the pavement may not represent measured deflections. They also reported that backcalculation of the modulus from surface deflections may yield conservative vertical compressive and radial tensile stresses.

Kim, Khosla, Satish, and Scullion (7) compared actual measurements of surface and depth

deflections and average vertical strains with predicted values. Forty-eight test sections on US-421 were instrumented with thermocouples, moisture probes, asphalt concrete strain gauges, and Linear Variable Displacement Transducers (LVDTs). Three drops using a FWD device were done. Surface deflections with FWD geophones and depth deflections with the LVDTs were measured. Values for the average vertical strain were also determined. The results verified that field measurements corresponded with theoretical values.

### **1.3 OBJECTIVES**

The objectives of the project were as follows:

- \* Develop a field instrumentation program for monitoring short and long term structural performance of a flexible pavement.
- \* Compare field results from non-destructive testing such as Falling Weight Deflectometer with data obtained from in-situ testing.
- \* Conduct a demonstration seminar on flexible pavement instrumentation and data collection procedures.
- \* Determine the influence of factors such as temperature, moisture content, and freezing on pavements.
- \* Compare the structural response of flexible pavement subjected to static and dynamic loading.



## CHAPTER 2

### INSTRUMENTATION AND INSTALLATION PROCEDURES

#### 2.1 PROJECT LOCATION

This project was located in West Central Ohio on State Route 33, east of the city of Bellefontaine, Logan County. The road was expanded from two lanes to four lanes. Six sections of a four mile stretch were instrumented. Instrumentation was completed in November of 1993. Environmental changes and dynamic loading response of the flexible pavement sections were recorded in December 1993 and data collection was completed in January of 1995. Monitoring was conducted in December, April, August, September, and January to document seasonal alteration.

#### 2.2 DESCRIPTION OF THE SECTIONS

Variance in the thicknesses of base with the different bases for each section are shown in Table 2.1. An asphalt concrete pavement of eleven inch thickness was placed over five different bases, each 8 inches of total thickness. Another section had thirteen inch thickness asphalt concrete over a six inch base. A description of the aggregate bases tested are given in Table 2.2.

Section 1 was a four inch, experimental, free-draining, Asphalt Treated Base (ATB) placed over a four inch standard 304 aggregate base.

Section 2 contained an experimental, cement-treated, free-draining base. Four inches of Portland Cement Treated Base (PCTB) overlies four inches of standard 304 limestone base.

Section 3 consists of four inches of New Jersey (NJ) base over four inches standard 304 limestone base. Of the bases tested NJ had the least amount of fines as shown in Table 2.2. NJ is a non-stabilized drainage base.

Table 2.1: Asphalt Thicknesses, Base Types and Thicknesses

Section	Station	Base Type	Base Thickness (inch)	Asphalt Thickness (inch)
1	954 + 50	Asphalt Treated	4	11
		304 Aggregate Base	4	
2	986 + 00	Cement Treated	4	11
		304 Aggregate Base	4	
3	1049 + 00	Non-Stabilized Drainage Base Type NJ	4	11
		304 Aggregate Base	4	
4	1056 + 00	Non-Stabilized Drainage Base Type IA	4	11
		304 Aggregate Base	4	
5	1115 + 00	304 Aggregate Base	8	11
6	1132 + 00	304 Aggregate Base	6	13

Table 2.2 Description of Non-Stabilized Base Materials

Sieve Size	Base Type					
	IA	NJ	304	IA	NJ	304
	Total Passing (ODOT)			Percent Passing (Specification)		
2 in.			100%			100%
1-1/2 in.			100%		100%	
1 in.	100%	100%	88%	100%	95-100%	70-100%
3/4 in.			75%			50-90%
1/2 in.	73%	74%	59%		60-80%	
3/8 in.						
No. 4		46%	49%		40-55%	30-60%
No. 8	24%	19%	32%	10-35%	5-25%	
No. 16		5%	24%		0-8%	
No. 30			18%			7-30%
No. 40						
No. 50	5%	3%	10%	0-15%	0-5%	
No. 70						
No. 200	3.5%	2.4%	6.4%	0-6%		0-13%

NJ (New Jersey) Non-Stabilized Free Draining Base  
 Proposed Aggregate Blend of 50% No. 6 Limestone,  
 37.5% No. 9 Limestone, and 12.5% Limestone Screenings

IA (Iowa) Non-Stabilized Free Draining Base  
 Proposed Aggregate Blend of 50% no. 6 Limestone,  
 33.5% No. 9 Limestone and 16.5% Limestone Screenings

Section 4 was an Iowa base type (IA). The IA non-stabilized drainage base is similar in composition to that of the standard 304 aggregate base. The difference between the two, as shown in Table 2.2, is that the IA contains less fine particles.

Sections 5 and 6 are standard 304 bases of eight and six inches thick, respectively. The total thicknesses of bases of Sections 1 through 5 are eight inches.

Each section was instrumented in the same manner and had the same cross-sectional plan as shown in Figure 2.1. Locations of instrumented sections were decided jointly by the Ohio Department of Transportation (ODOT) and Center for Geotechnical and Environmental Research (CGER) personnel. All sections instrumented were in the east-bound driving lane. Driving and passing lanes were 12 feet wide. Berms along the driving and passing lanes were 10 feet and 4 feet wide, respectively.

### **2.3 INSTRUMENTATION SELECTION**

The foremost concern of this project was to ensure that the instrumentation selected could endure installation and environmental factors and still perform within the sensitivity range. The instrumentation was expected to survive elevated temperatures, compaction, moisture, and repeated heavy loading. High temperature (200-300°C) at installation and saturated moisture conditions over an extended time period were particular concerns. Instrumentation was selected to monitor the following: 1) pressure between the base and the subgrade material; 2) pressure between the pavement and base material; 3) deflection of the pavement in the wheelpath; 4) volumetric moisture content of the base and subgrade material; 5) temperature profile of the pavement; and, 6) strain measurement from FWD loads.

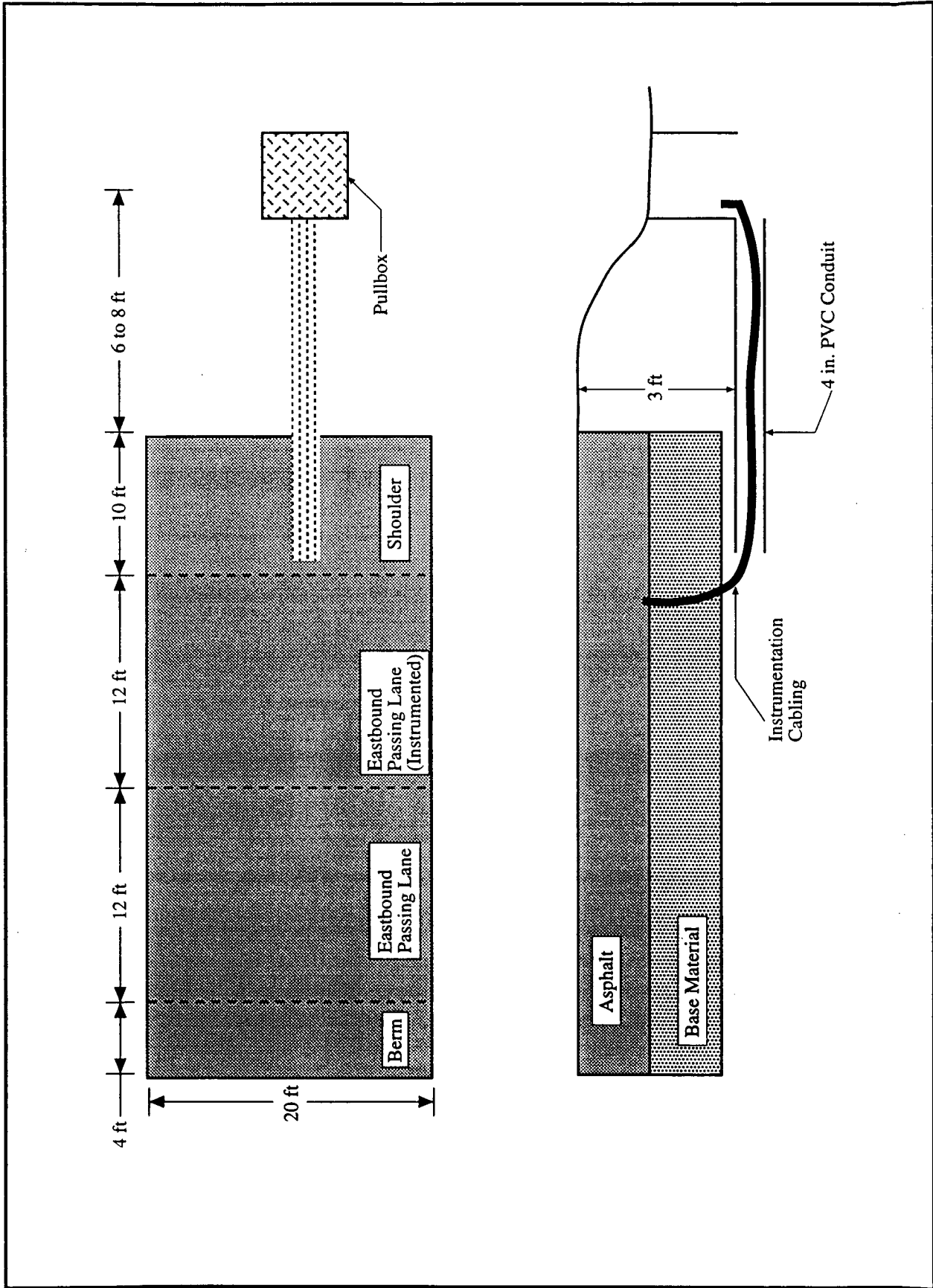


Figure 2.1 Plan and Cross-Sectional Views of a Typical Instrumentation Site.

### 2.3.1 Strain Measurement

The strain in the pavement was measured along the wheelpath by two different types of strain gauges: Dynatest PAST-IIAC strain gauge, and the Hottinger Baldwin Messtechnik (HBM) DA 3 encapsulated strain gauge. Careful installation of each gauge was made to ensure desired bonding of the asphalt concrete and gauge to obtain an accurate reading. Service life was expected to exceed three years.

The Dynatest PAST-IIAC strain gauge is distributed by Dynatest Consulting, Inc., of Ojai, California. This gauge operates as a 120-ohm quarter Wheatstone bridge with a temperature range of -30 to 150°C, and a gauge factor of 2.00. It has a range of 1500 micro-strain and a service life greater than 36 months. The PAST-IIAC gauge is an H-type gauge. It is coated with an epoxy-silicone-titanium coating by means of a multi-layer "coating" process to provide good bonding and protection against mechanical and chemical deterioration. The gauge is completely embedded in a strip of glass-fiber reinforced epoxy, a material with low stiffness, good flexibility and strength. Each end of the epoxy strip is fastened to a stainless steel anchor for ample bonding to the asphalt concrete. The gauge measures 132 mm in length and 6 mm thick with two 75 mm arms.

The HBM DA 3 strain gauge is distributed by Hottinger Baldwin Measurements, Inc., of Marlboro, Massachusetts, and operates on a 350-ohm quarter bridge. This gauge measures 88 mm in length with a thickness of 1.2 mm. Its operating temperature range is -50 to 70°C and has a varying gauge factor of approximately 2.11. This gauge, encapsulated in poly-carbonate, is mainly used for strain measurement in asphalt concrete and must be installed at a temperature less than 120°C.

### 2.3.2 Deflection Measurement

Deflection of the asphalt concrete was measured using accelerometers and Linear Variable Displacement Transformers (LVDTs). The accelerometers were positioned in the asphalt concrete. The LVDTs measured deflection when placed in a Single Layer Displacement (SLD) unit, as shown in Figure 2.2. The reference rod is sunk deep enough (10 ft.) so displacement at that depth due to surface loading is negligible in the deflection measurement. Based upon field measurements and elastic theory, reference rods should be anchored not less than 6 ft. from the subgrade. The reference rod is then assumed to be stationary while the LVDT monitors the pavement as it deflects. The SLD has the advantage over the accelerometer in that it can measure both static and dynamic deflection as well as permanent deformations.

The LVDTs are manufactured by Schlumberger Industries of Buffalo, New York. The LVDTs used were a DC type, spring loaded. They are submersible in any liquid not corrosive to their stainless steel construction. Each LVDT has a linear stroke of  $\pm 15$  mm and a sensitivity of approximately 2.8 mm/volt, varying for each LVDT. They have an operating temperature range of -20 to 80°C and operate at 10V DC excitation. While enclosed in the SLD, the armature of the LVDT rests on an anchored reference rod at four different depths for each section. This arrangement measures deflection of the anchor point relative to the pavement. Response is measured by a change in voltage over a linear range of  $\pm 5$  volts. All LVDTs were calibrated using a digital micrometer and software from the data acquisition system that correlated the output voltage with measured displacement. The calibration factor was determined in inches/volt. Each LVDT was calibrated several times to verify that the calibration factor was repeatable to within 1%. It was discovered through the course of the project the LVDTs were inoperative at temperatures below freezing

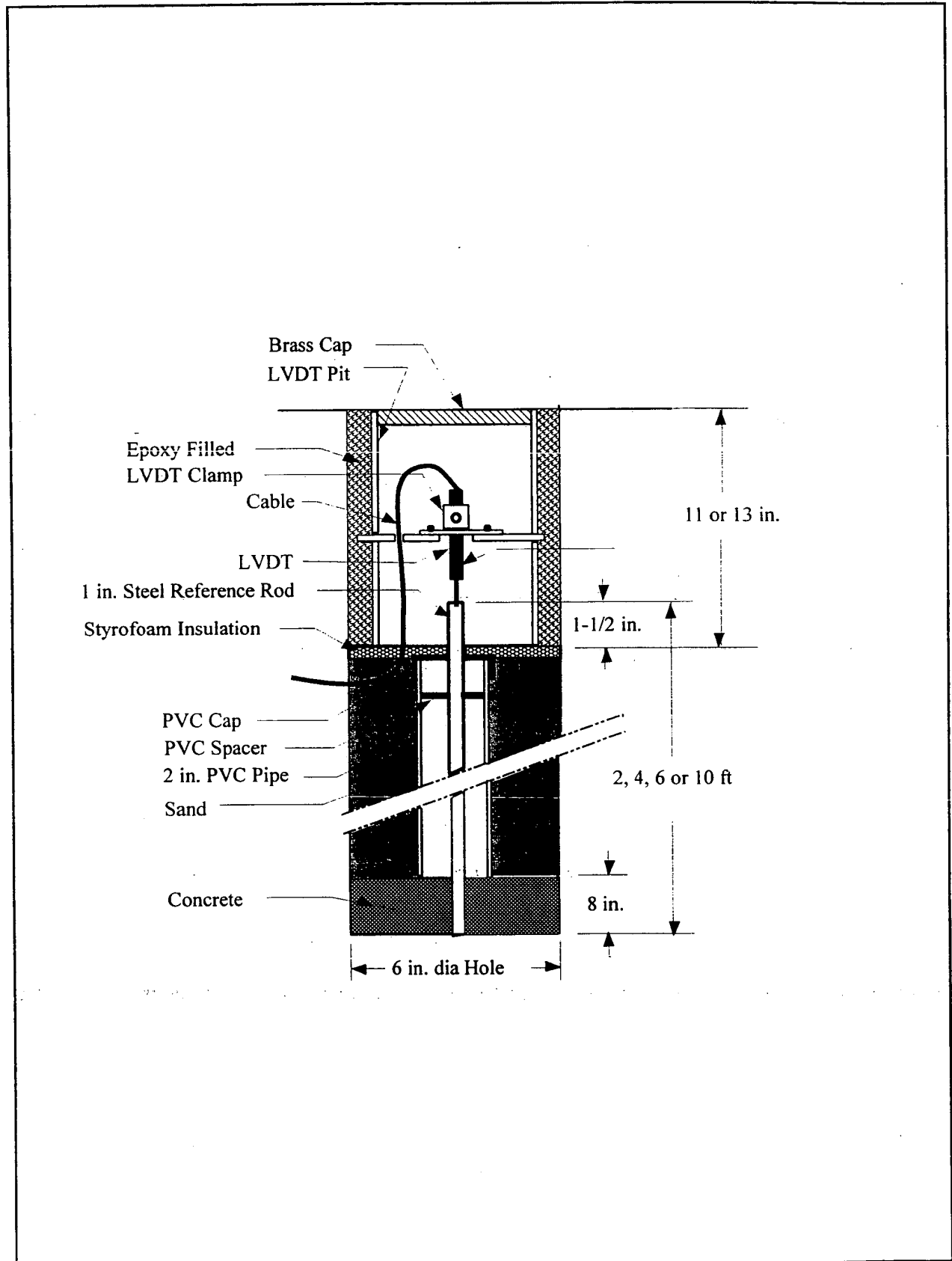


Figure 2.2 Single Layer Deflectometer (SLD) Construction

because moisture will freeze and prevent the LVDT plunger from moving.

The accelerometers selected for this project were distributed by Measurement Instruments East, Inc., of Blairsville, Pennsylvania. The model 793L Piezoceramic accelerometer is made of lead-zirconate titanate. The accelerometers have a frequency range of 0.4 to 1000 HZ and an output range of up to 500 mV/G. They have a charge sensitivity of 350 PicoCoulombs per Newton (pC/N) and have been used successfully at temperatures exceeding 260°C. Service life is expected to be in excess of three years.

### **2.3.3 Moisture Measurement**

The volumetric moisture content of the soil was measured using a system developed by Campbell Scientific, Inc., of Logan, Utah. The system uses Time Domain Reflectometry (TDR) to measure the soil moisture. This is a process of sending pulses along a coaxial cable to two parallel, 12 inch, stainless steel rods embedded in the soil and observing the velocity of the reflected waveform. The velocity of a waveform traveling down a coaxial cable or waveguide is influenced by the type of material surrounding the conductors. If the dielectric constant of the material is high, the signal propagates slower. Because the dielectric constant of water is much higher than (about 80 in water versus 0 in air), a signal within a wet or moist soil propagates slower than in the same soil when dry. Thus, moisture content can be determined by measuring the propagation time over a fixed length probe embedded in the soil beneath the pavement.

### **2.3.4 Temperature Measurement**

Thermocouples are commonly used sensors for monitoring pavement temperature. Single point thermocouples, distributed by Measurement Instruments East, Inc., of Blairsville, Pennsylvania, were used on this project. Thermocouples were placed in the top and bottom layers

of the asphalt concrete (the same layers as the strain gauges) and at the subgrade/base interface. Each thermocouple was sealed in a stainless steel tube for protection from moisture and high temperature of the asphalt concrete during installation.

### **2.3.5 Interface Pressure Measurements**

Two types of pressure cells, distributed by GEOKON, Inc., of Lebanon, New Hampshire, were used to measure the vertical stresses under the pavement. Model 3650 strain gauge pressure cells, and the Model 4800E vibrating wire pressure cells, were selected. Both types of pressure cells were used to measure the pressure changes between the base and subgrade interface, and also the pressure changes between the pavement and base. The strain gauge pressure cells were used to measure the pressure changes caused by both the static and dynamic loading. The vibrating wire pressure cells were only used for static loading conditions. Both cells consist of two 9 inch circular stainless steel plates, welded together and spaced apart by a narrow cavity filled with an antifreeze solution. External pressure acting on the cell is read by a data acquisition system. Both cells have an operating range of 0-30 psi.

The calibration numbers for the pressure cells were supplied by GEOKON. These numbers were obtained using a hydrostatic system that calibrated the pressure sensor. For this project there were two calibration procedures, a uniaxial and a hydrostatic calibration. A uniaxial calibration best simulates conditions where load is transferred directly to the soil. However, the actual field loading is very complex and is difficult to simulate as field conditions are constantly changing. Since the hydrostatic calibration more closely corresponded to the calibration numbers given by Geokon, these numbers were used here.

## 2.4 INSTRUMENTATION LAYOUT

The sensors were placed in the asphalt concrete where the largest values of strain, deflection, and pressure would occur. In all instrumented sections, sensors were installed in a straight line along the wheelpath of the driving lane. Figure 2.3 shows the position of the various types of instrumentation in the plan and cross-sectional views of a typical section.

The LVDTs were installed along the wheelpath. The reference rods varied in depth for each SLD assembly unit. The depths for each reference rod for the four LVDTs were 10, 6, 4, and 2 feet, respectively. Different depths were used in order to compare the deflection of the pavement, referenced at the mid-point of different soil layers.

All strain gauges were installed at two depths within the asphalt concrete. The first level of gauges was located 1 inch from the bottom of the pavement. The second level of gauges was located 1 inch from the top of the pavement. Gauges were spaced at a distance of 2½ feet apart along the wheelpath. After the final layer of pavement was laid in the summer of 1994, the top gauges were at a depth of approximately 2¼ inches from the top of the asphalt concrete.

Earth pressure cells were installed at two interfaces: at the subgrade and base interface and at the pavement and base interface. The pressure cells were placed along the wheelpath, aligned vertically within their respective layers. This installation was followed for both types of pressure cells.

The moisture content was monitored at two locations: at a depth of 6 inches from the top of the subgrade and at the mid-point of the base layer. The moisture probes were located at a depth of 4 inches below the top of the base layer since the thickness of the base was approximately 8 inches. Soil moisture probes were located along the wheelpath with probes aligned horizontally.

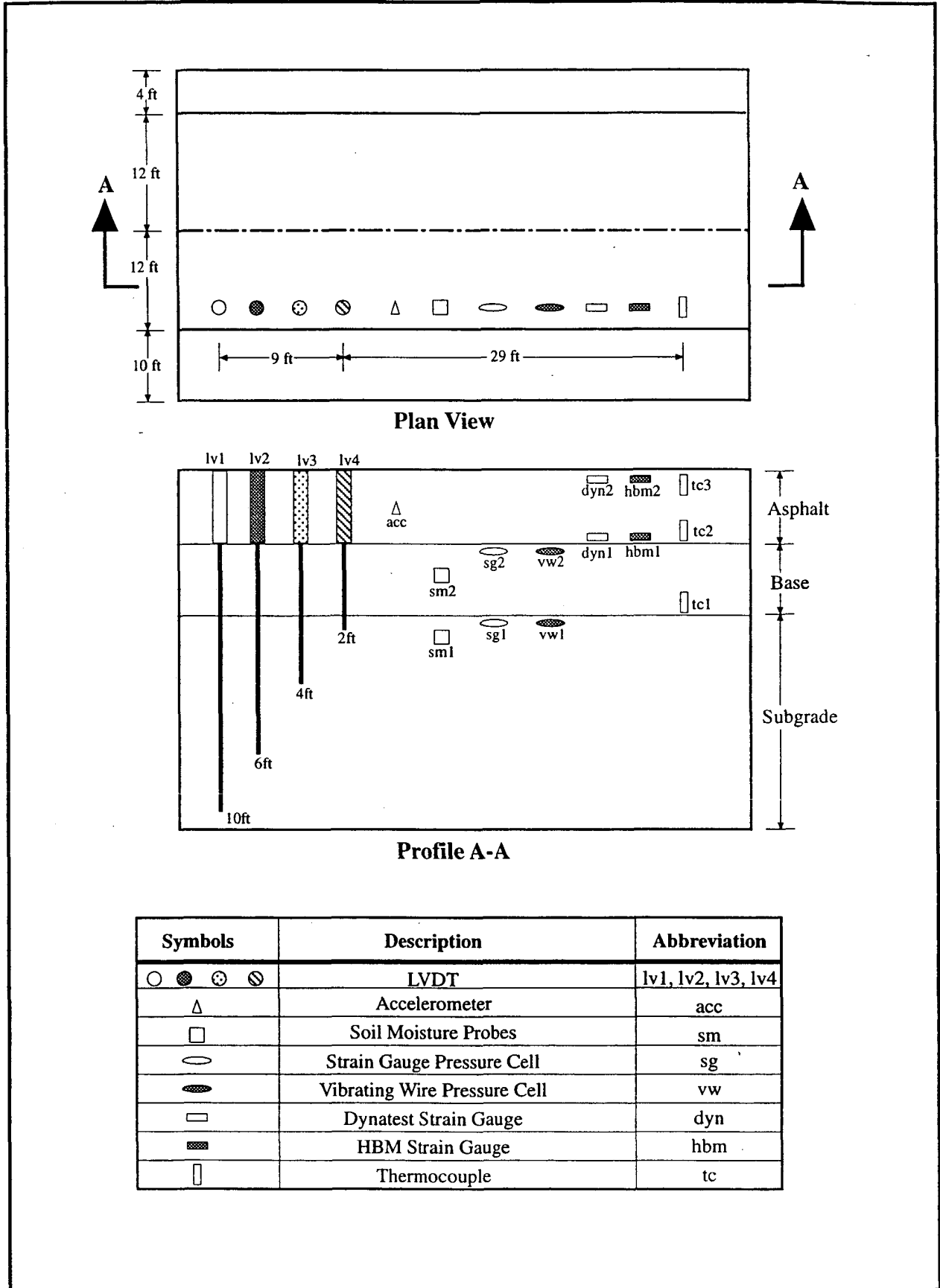


Figure 2.3 Typical Instrumentation Location

## **2.5 SENSOR INSTALLATION**

The installation of sensors into pavement test sections was a crucial part of the project. Each section of the test road was instrumented with strain sensors, pressure cells, thermocouples, moisture probes, accelerometers, and displacement transducers. The principal concerns were that sensors should stay in position and remain functional after paving. Sensors had to successfully resist the lateral force the paver exerted, survive the vertical compaction, and survive the high temperature of asphalt concrete during placement.

### **2.5.1 Soil Moisture Probes**

In order for the soil moisture probes to be installed in the subgrade material, a hole approximately 6 inches deep, 3 inches wide, and 15 inches long was excavated. The two 12 inch stainless steel probes were placed parallel to each other 6 inches apart in the hole. The excavated subgrade material was replaced with probe placement and then compacted. This step was completed the day before the base was installed. After the base was installed, the same procedure was used to place the probes in the base material. The depth of the hole was 4 inches in order for the probes to be in the center of the base material. For Sections 1 and 2, moisture probes were installed in the subgrade and in the 304 material immediately below the treated bases. The cables attached to the probes were buried along the top of the respective material and directed toward the center of the section and then outward. A moisture resistant junction connected lead cables from the probes to a main cable which ran to the pullbox. Sand was placed around the junction to cushion it from the surrounding aggregate.

### **2.5.2 Earth Pressure Cells**

Pressure cells were installed in two different locations: 1) subgrade-base interface, and 2)

base-pavement interface. The installation procedure was the same in both locations. The pressure cell was placed flush with the top of the layer with no aggregate irregularities in contact with the sensitive contact surface. First, the subgrade or base material was excavated approximately 2 inches in depth at the installation region. Then a layer of sand was placed in the excavated hole. The pressure cell was then placed in the hole, sensitive surface down, and covered with a layer of sand. The cable connected to the transducer was buried along the top of the subgrade or base towards the center of the section and then towards the berm.

### **2.5.3 Single Point Thermocouples**

Thermocouples were positioned at the same depth as the other sensors. A 1 inch layer of either base or asphalt concrete material was placed under the thermocouple to obtain the desired height. The thermocouple was then placed in a horizontal position and covered with the same material. The cable from the thermocouple assembly was laid towards the center of the section and then run outward. Asphalt concrete was placed on top of the cable to keep it from moving during paving.

### **2.5.4 Single Layer Deflectometers (SLD)**

The SLD assembly was installed after paving. It consisted of an LVDT attached to a steel housing and epoxied into the pavement above a fixed reference rod. The deflection of the pavement was measured by the SLD unit relative to a point fixed at various depths below the road surface.

The LVDT housing was fabricated using a 4 inch diameter, 1/4 inch thick steel pipe, a 3-1/2 inch steel coupling, and a 3/8 inch thick steel plate. The steel plate was used to mount the LVDT inside the housing and to anchor the housing to the pavement when bonded with epoxy. A stainless steel clamp was constructed to hold the LVDT firmly to the steel mounting plate above the reference

rod. The clamp utilized a set screw to secure the LVDT so that it could be adjusted, removed, or recalibrated after installation. The housing was capped with a 3-1/2 inch brass plug that was removed to access the LVDT whenever needed.

Since the asphalt concrete was placed in layers, all the cabling had to be installed prior to paving. Cables were laid out in the subgrade material at their respective positions. A 2 foot long piece of 2 inch diameter PVC pipe was cut and placed at each LVDT location. The PVC pipe held the extra wire needed to connect to the LVDT. The end of the PVC pipe was placed exactly 30 inches from the edge of the road (wheelpath). When paving was finished, a hole was cored and the wire accessed. The location of PVC pipes was extremely important. Once the paving was complete, a coring machine was brought in by ODOT. A 4 inch diameter core was made at all four LVDT locations. Holes were then augured to the four different depths of 2, 4, 6, and 10 feet below the surface of the base material. Each of these holes would contain one SLD assembly.

After the hole was cored, the cable was located at the end of the PVC pipe and pulled up to the top of the hole. The bottom of the hole was tamped with the end of a spud bar to compact any loose soil. The reference rod was set in the center of the hole and driven down so that approximately 2 inches of the rod remained above the top of the base material, into the asphalt concrete layer, so that the LVDT plunger rested on the end of the rod inside the housing. Reference rods were grouted at the selected depth. A 2 inch diameter PVC pipe was placed over the rod to keep subgrade material away from it. A machined PVC spacer was used at the rod top to dampen rod vibrations and center the reference rod within the PVC pipe. The hole was then backfilled with sand to the top of the base layer.

Before pouring the epoxy around the housing, brass caps were installed on the top of the

housings to keep the excess epoxy from entering the housing and to provide a smooth transition of traffic across the top of the SLDs (Figure 2.4). The epoxy was then carefully poured around the SLD assembly (Figure 2.5). Once the epoxy had cured, the brass caps were removed to make sure that the epoxy didn't seep under the housing or "freeze" the cap to the top of the housing. All twenty-four LVDT housings were found to be centered above their respective reference rods and flush with the top of the asphalt concrete. After inspection of the housings, the LVDTs were set at zero.

#### **2.5.5 Strain Gauges (Dynatest, HBM)**

The survivability of the gauges was the first priority during installation. Since all the strain gauges were installed along the wheelpath at the same depth, the installation procedure for each gauge was similar. After the position for the gauges was laid out, asphalt concrete was taken from the paver, sieved through a custom made sieve, and placed at each gauge position. Once the desired height was reached, the gauges were placed in position and covered with more sieved asphalt concrete to prevent aggregate in the asphalt concrete from contacting the sensor. The asphalt concrete was then compacted by placing a board over the gauges and applying a static load. The wire connected to the gauges was pulled towards the center of the section and then outward towards the berm. Asphalt concrete was also put over the wires to keep them in place during the paving process. Placing the asphalt concrete over the gauges approximately 5 minutes before the paver arrived ensured that the asphalt concrete would still be hot.

#### **2.5.6 Instrumentation Cabling and Labeling**

The majority of the instrumentation used on the project was purchased with a sufficient length of lead cable to reach the pull boxes. Instrumentation with short lead wires was spliced with direct burial cable and sealed with several layers of waterproof heat shrink to protect from moisture.

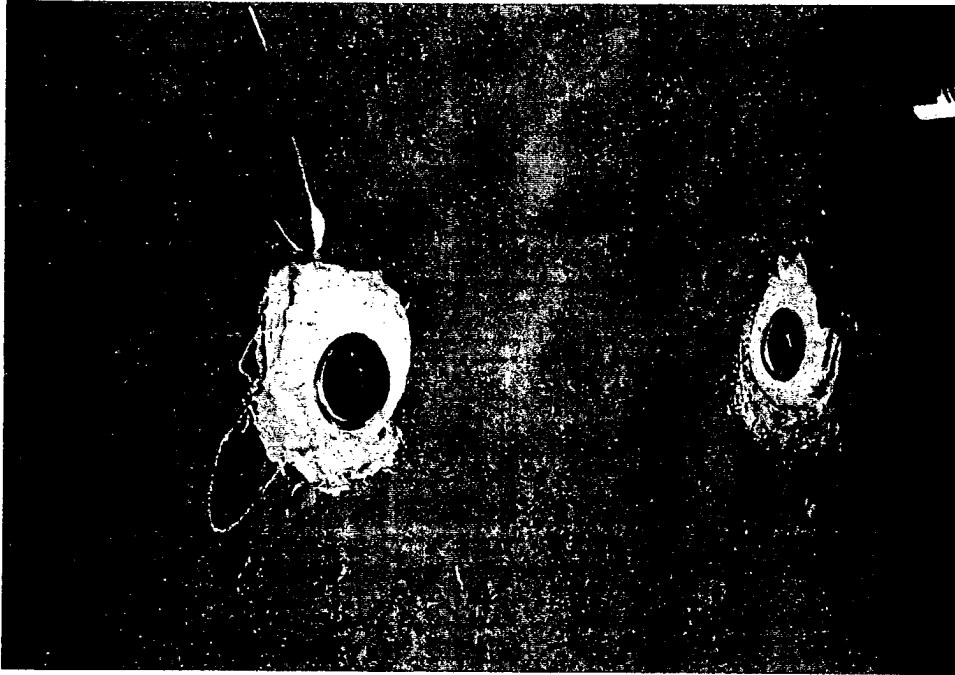


Figure 2.4 Exposed Brass Cap of the Single Level Deflectometer



Figure 2.5 Epoxy Used to Fix Single Level Deflectometer Unit

Both types of strain gauges required additional lead cable.

All instrumentation cabling converged and exited from the center of each section. To prevent the cables from being cut by the finish grader, the pavement was chipped back approximately 6 inches. This additional step became necessary after all the cabling in section 5 was cut, although it was clearly marked by fluorescent spray paint. Once the cables exited the pavement, they were buried approximately 2 feet below the expected grade line and enclosed in 4 inch PVC pipe from the edge of the pavement to the pull box.

All the instrumentation cables were marked with a unique label to identify each gauge and to determine its position. A typical label read: S2DYN01. The first letter and number refer to the section where the sensor is located. The next set of letters describes the type of gauge, while the last two numbers gives the gauge's location in the pavement. This particular example illustrates that this is a Dynatest gauge located in Section 2 and is the first gauge installed, which means it is in the bottom layer of the asphalt concrete.

### **2.5.7 Instrumentation Location Reference**

A coordinate system was established prior to placing any of the base material or paving any part of the road. This was crucial to ensure that all the gauges were placed along the wheelpath and that each layer of instrumentation was located accurately.

After the stations for each section were determined, an ODOT surveying crew marked the center line of the road to establish the wheelpath location. A line was strung across the road at two consecutive station markers and tied off on stakes (i.e., Station 1049 + 00 and 1049 + 50). The wheelpath was measured along these lines referencing the ODOT surveyed centerline. The

wheelpath was then marked in the road. Since sections were 29 feet long, another line was stretched between these two wheelpath marks connecting the lines of the two consecutive station markers. A straight line was painted on the roadway. This line marked the wheelpath. Next, a measurement of 29 feet was marked on the wheelpath measuring from the first station, which was the beginning of the section. Two other lines were strung up connecting the consecutive station markers on the edge of the road and a measurement of 29 feet from the first station was marked. This would place a rectangle around the section. Finally, marks were made 2 feet from each of the four corners of the rectangle measured away from the road. This is where the 2 foot long, 1 inch diameter steel reference pins were placed. Holes for the reference pins were dug with posthole diggers at a depth of approximately 4 feet. This placed the pins well below the proposed final grade. The pins were driven in the ground approximately 8 inches and then grouted with 8 inches of concrete. All reference measurements were taken from the pins to locate sensors. As pins became buried, they were located by the use of a metal detector and uncovered.

This layout scheme worked very effectively in that all the gauge locations were easily found and gauges were installed in the wheelpath of the pavement as planned. The accuracy of the reference layout was verified when all 24 wires were located for the LVDTs.



## CHAPTER 3

### TESTING PROCEDURE AND DATA COLLECTION

#### 3.1 TESTING

Non-Destructive Testing (NDT) has become an important tool for measuring response of pavement to a known load (8). The Falling Weight Deflectometer (FWD) was chosen for this project. An impulse load is generated by means of a mass falling onto a circular plate where the shape of these loads simulate loading that is applied to pavement by traffic. Measured deflections, collected from the FWD, were compared with data collected from sensors installed in the pavement.

##### 3.1.1 FWD Testing Equipment

Large amounts of data had to be collected from multiple channels in small increments of time to enable comparison of results. The data acquisition system used was comprised of a 486/25 IBM compatible personal computer, a 16 channel analog to digital (A/D) plug-in interface with accompanying software, signal conditioners/amplifiers for each channel, and the Enhanced Graphics Acquisition and Analysis (EGAA) software package, developed by R.C. Electronics of Golet, California. Figure 3.1 shows the data acquisition equipment used.

The 16-channel A/D interface can record up to 16 separate instruments simultaneously, with up to 2000 samples per channel per second. The input range of the A/D board is  $\pm 10$  volts. With the 16-channel A/D interface, the system has a special feature which enables the user to sample and hold the input signal from the instrumentation. During the test the data collected was examined to determine if data would be useful and if the sensor was responding correctly.

The sensor signals were run through a sensitive, high speed signal conditioner/amplifier before the data were recorded. This conditioner/amplifier was used to place a specific gain on each

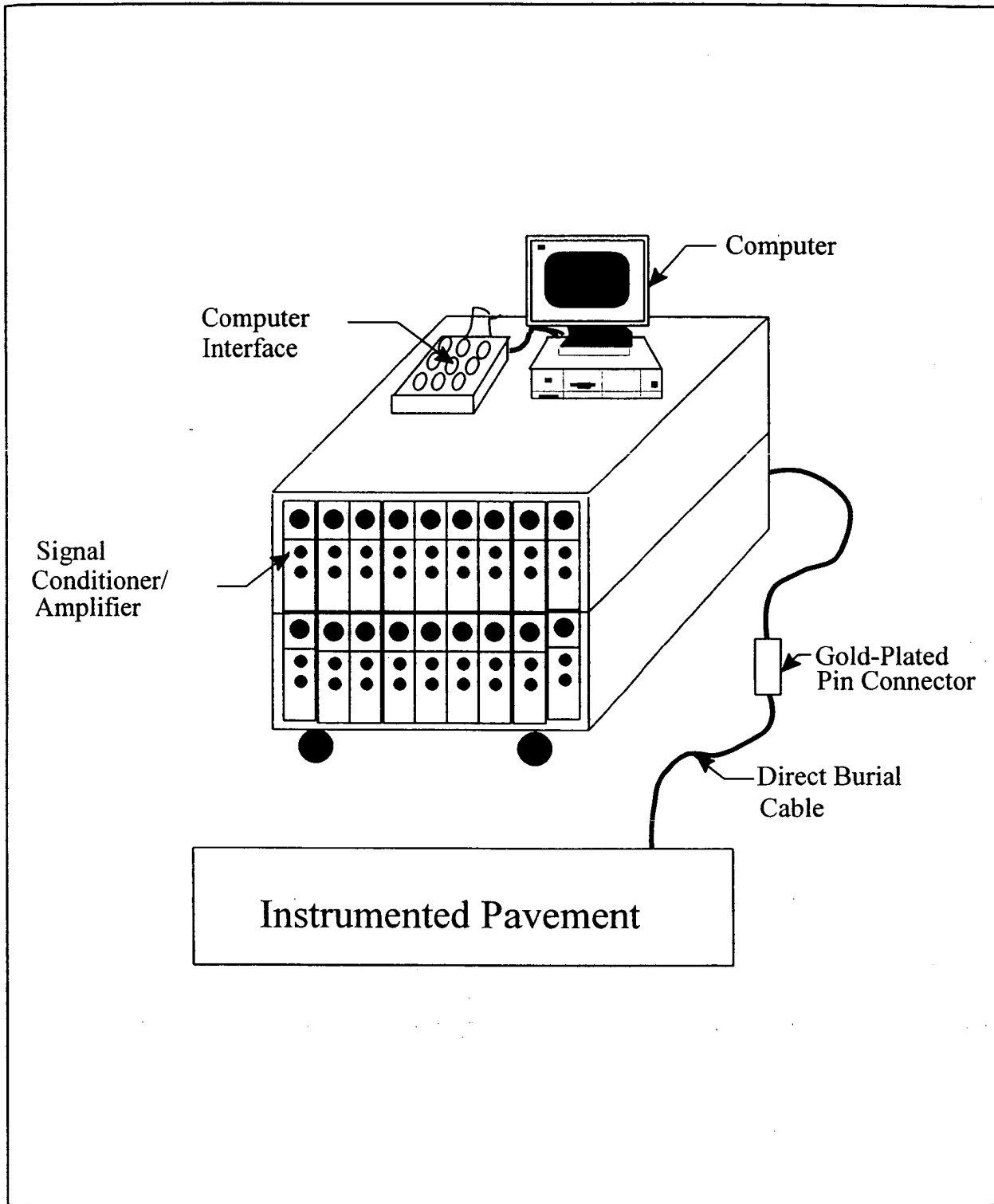


Figure 3.1 FWD Data Acquisition Equipment

instrument to amplify the signal so that the maximum amount of the signal from each instrument could be obtained.

The conditioner/amplifier and an external power supply were used to provide excitation voltages to the instrumentation. The Dynatest and the HBM strain gauges received an excitation voltage of 1.75 volts, while the SLDs received an excitation voltage of 12 volts. The semi-conductor pressure cell was supplied with an excitation voltage of 28 volts.

### **3.1.2 Testing Procedure**

The Dynatest Model 8000 Falling Weight Deflectometer applied an impact load to the pavement with an applied pressure in the range of 140 to 175 psi. Before each drop of the falling weight, seven geophones were lowered and placed on the pavement surface so that the surface deflection could be measured during each drop. The deflections were measured at 0, 8, 12, 18, 24, 26, and 60 inches away from the center of the loaded area. After test completion, a copy of all data was printed for the drops made, along with the air temperature, all seven deflection measurements, the applied load pressure and exact load equivalent, station number, time of day, and gauge name where the load was applied. Figure 3.2 shows a sample printed copy.

Three drops were applied to the instrumentation during each of the FWD tests. The instrumentation included the strain gauge pressure cells, accelerometers, LVDTs, and the Dynatest and HBM strain gauges. Their responses were monitored by the EGAA system. The EGAA system had to be manually triggered to capture the instrumentation response. The sample frequency was used to capture 2000 sample points per second. The trigger operation had to activate the system within 1 second of the impact of the load on the pavement to ensure that the sensor response was collected.

09:19 940926

2.

File: A:\4603394C  
Road: LOG US33  
Subsection: FLEXIBLE

FWD S/N : 8002-036  
Operator ID : RDM

Stationing...: Manual Input

Diameter of Plate: 11.8  
Deflector distances : 8 12 18 24 36 60

OHIO UNIVERSITY TING (S1,S3) - HIGH LOAD FOR D1 < 60 MILS  
Sequence: 4

'BEGIN TESTS IN SECTION #1

Stn: 1LV01	Lane:4/4	Temp: 62	J/C:							09:54
Sto Hgt	psi	lbf	Df1	Df2	Df3	Df4	Df5	Df6	Df7	
* 4	155.1	17000	12.47	10.49	9.44	8.09	6.83	4.95	2.43	

Stn: 2LV01	Lane:4/4	Temp: 62	J/C:							09:54
Sto Hgt	psi	lbf	Df1	Df2	Df3	Df4	Df5	Df6	Df7	
* 4	154.6	16952	12.39	10.45	9.40	8.04	6.83	4.95	2.48	

Stn: 3LV01	Lane:4/4	Temp: 62	J/C:							09:55
Sto Hgt	psi	lbf	Df1	Df2	Df3	Df4	Df5	Df6	Df7	
* 4	155.2	17016	12.27	10.53	9.31	8.00	6.79	4.91	2.43	

Stn: 1LV02	Lane:4/4	Temp: 62	J/C:							09:58
Sto Hgt	psi	lbf	Df1	Df2	Df3	Df4	Df5	Df6	Df7	
* 4	153.2	16800	18.75	10.86	9.81	8.37	7.04	5.20	2.48	

Stn: 2LV02	Lane:4/4	Temp: 62	J/C:							09:59
Sto Hgt	psi	lbf	Df1	Df2	Df3	Df4	Df5	Df6	Df7	
* 4	156.4	17144	18.15	10.65	9.65	8.25	6.99	5.16	2.48	

Stn: 3LV02	Lane:4/4	Temp: 62	J/C:							10:00
Sto Hgt	psi	lbf	Df1	Df2	Df3	Df4	Df5	Df6	Df7	
* 4	155.1	17008	18.55	10.57	9.60	8.21	6.95	5.16	2.48	

Stn: 1LV04	Lane:4/4	Temp: 62	J/C:							10:02
Sto Hgt	psi	lbf	Df1	Df2	Df3	Df4	Df5	Df6	Df7	
* 4	150.7	16520	21.97	10.45	9.35	7.88	6.63	4.70	2.35	

Stn: 2LV04	Lane:4/4	Temp: 62	J/C:							10:02
Sto Hgt	psi	lbf	Df1	Df2	Df3	Df4	Df5	Df6	Df7	
* 4	151.3	16584	21.12	10.24	9.15	7.76	6.54	4.66	2.35	

Stn: 3LV04	Lane:4/4	Temp: 62	J/C:							10:03
Sto Hgt	psi	lbf	Df1	Df2	Df3	Df4	Df5	Df6	Df7	
* 4	150.7	16536	21.65	10.12	9.06	7.68	6.54	4.62	2.31	

Stn: 1ACC01	Lane:4/4	Temp: 62	J/C:							10:04
Sto Hgt	psi	lbf	Df1	Df2	Df3	Df4	Df5	Df6	Df7	
* 4	150.9	16536	11.51	9.91	8.90	7.60	6.42	4.49	2.22	

Stn: 2ACC01	Lane:4/4	Temp: 62	J/C:							10:05
Sto Hgt	psi	lbf	Df1	Df2	Df3	Df4	Df5	Df6	Df7	
* 4	152.0	16664	11.23	9.70	8.73	7.52	6.34	4.49	2.22	

Stn: 3ACC01	Lane:4/4	Temp: 62	J/C:							10:06
Sto Hgt	psi	lbf	Df1	Df2	Df3	Df4	Df5	Df6	Df7	
* 4	152.0	16664	11.15	9.74	8.56	7.35	6.26	4.41	2.31	

Stn: 1SGFC01	Lane:4/4	Temp: 62	J/C:							10:07
Sto Hgt	psi	lbf	Df1	Df2	Df3	Df4	Df5	Df6	Df7	
* 4	152.2	16680	11.87	10.28	9.15	7.84	6.59	4.66	2.35	

Figure 3.2 FWD Deflection Printout

Four sets of FWD testing were conducted on the project from December of 1993 through January of 1995. The first test involved only the first four sections of the project due to construction on the existing two lanes near sections 5 and 6. This was also the case for the second test in April of 1994. But for the last three tests in August and September of 1994, and January of 1995, all the sections were available for testing. The eastbound driving lane of the newly constructed road was closed to traffic until the completion of the FWD test.

## **3.2 ENVIRONMENTAL DATA**

The condition of the pavement and base materials at the time of testing must be known to obtain a complete comparison of the data throughout the different seasons. While collecting the data from the FWD tests, the temperature from the top and the bottom of the pavement, as well as the temperature of the base material was recorded. In addition, volumetric moisture content of the subgrade and base material were recorded.

### **3.2.1 Testing Equipment**

The Omega Model HH21 Microprocessor Thermometer was used to measure the temperature of the pavement and base material. This is a hand held device that allows the lead wires of the thermocouples to be connected directly to terminals. This unit was powered by a 9 volt battery and read the temperature to an accuracy of  $\pm 0.1$  degree. The reading was displayed on an LED screen on the top of the instrument and recorded manually.

The Campbell Scientific datalogger and Tektronix 1502B cable tester, along with a Toshiba T3100 laptop computer were used to monitor the soil moisture content. The Toshiba T3100 was used to download the commands to start up the system and the values of the moisture content were

read and recorded directly from the screen. The Tektronix 1502B sent the actual pulse down the coaxial cable that was used to determine the moisture content in the soil.

### **3.2.2 Testing Procedure**

The soil moisture content and temperatures were collected during each of the falling weight tests. The soil moisture probes were hooked up first so that the Campbell system could initialize itself and take the moisture readings. After the system was initialized, the displayed moisture results were recorded on field notes for the section being tested. While the soil moisture was being read, each thermocouple was connected to the Omega HH21 and their corresponding temperatures were recorded in the field notes, along with the soil moisture. This process took approximately 10 minutes per section. As was fully described previously, all instrumentation cables for each section were centrally available and individually coded at each section's pull box.

## **3.3 SUMMARY OF ALL SENSOR LOSSES**

Since most of the gauges are highly sensitive, extreme care must be taken during installation. Proper installation technique and data collection practices can minimize errors in data. However, since the installation procedures utilized in this project were new, some problems and losses were encountered. The condition of sensors at the completion of testing is shown in Table 3.1.

### **3.3.1 Instrumentation**

It was discovered through the course of the project that the LVDTs were inoperative at temperatures below freezing. This was due to moisture freezing the core to the coil housing, resulting in zero voltage change. When the core was heated, the LVDTs functioned normally. The 10 ft. depth LVDT data was not available for Section 6 as the rod fell from the LVDT contact during

Table 3.1: A List of Sensors Still Working at Completion of Project

Section	Functional	Non-Functional
1	ACC HBM01 LVDTs SGPC01/02 SM01/02 TC01/02/03 VWPC02/01	DYN01/02 HBM02
2	ACC DYN01/02 HBM01/02 SGPC1/02 SM01/02 TC01/02/03 VWPC01/02	
3	ACC HBM01 LVDTs SGPC01/02 TC01/02/03 VWPC01/02	DYN01/02 HBM02 SM01/02
4	ACC DYN01 HBM01/02 LVDTs SGPC01/02 SM01/02 TC01/02/03 VWPC01/02	DYN02
5	ACC DYN01 LVDTs SGPC01/02 SM01/02 TC02/03 VWPC01/02	DYN02 HBM01/02 TC01
6	ACC DYN01/02 HBM01 LVDT 02/03/04 SGPC01/02 SM01/02 TC01/02/03 VWPC01/02	HBM02 LVDT01

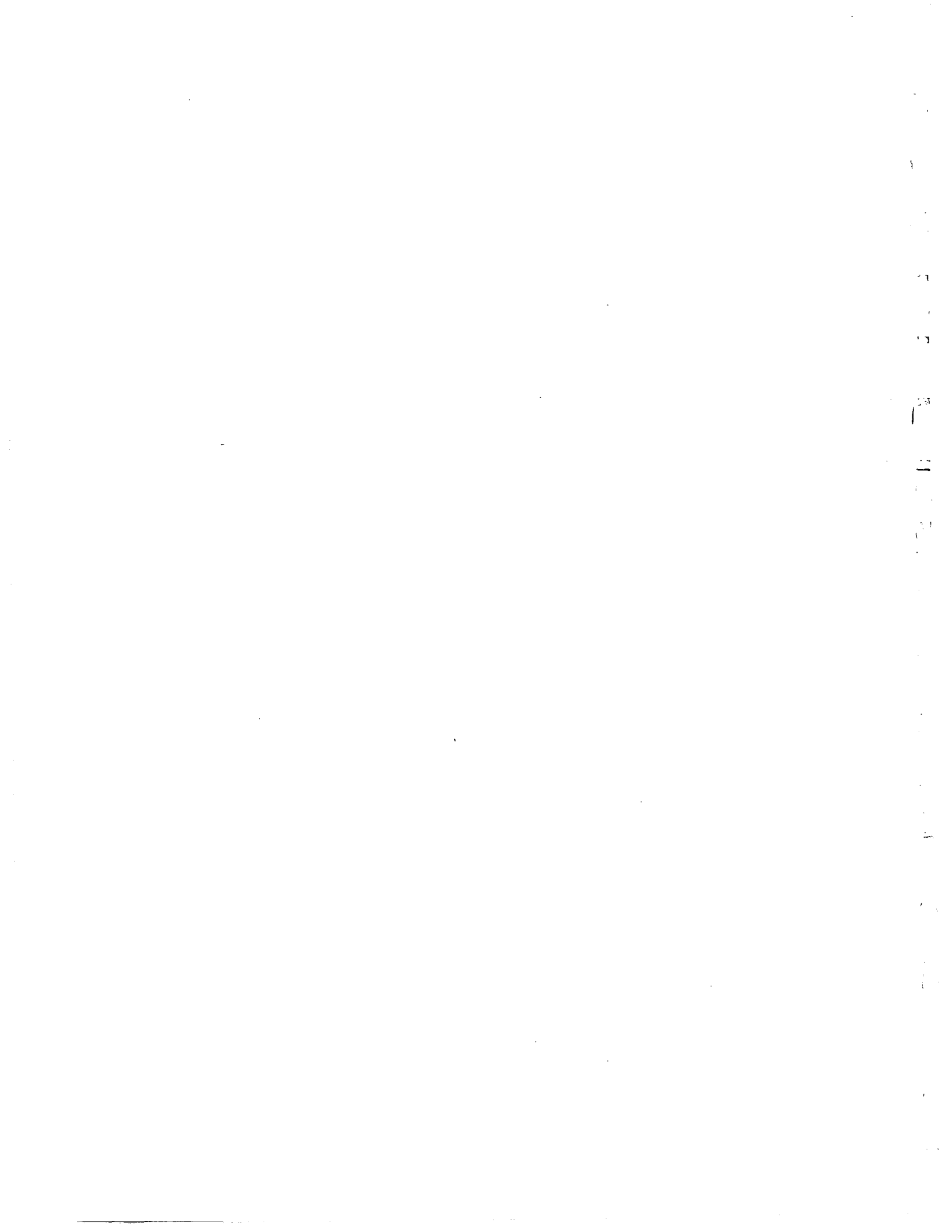
installation. Attempts to adjust the contact point failed to give reliable readings.

The Dynatest gauge located at the top of the pavement, for Section 1, was lost due to the burning of the outside covering of the gauge by hot asphalt concrete when the paver stopped on top of the gauge. The bridge balance was found to be out of the amplifier range. The HBM gauges, for Section 2, did not respond during the January test. The top HBM gauge did not respond in April. Prior to the April test, for Section 3, the wiring to all instrumentation was cut while power lines to the section were being laid. The HBM gauges were spliced to their original wiring. The Dynatest gauges, however, could not be spliced together and produced no data during further testing. Although strain data was collected for the remaining gauges, because of the splices, the readings may not be accurate. There was not sufficient data to plot the top Dynatest gauge. In Section 4, the top Dynatest gauge was nonresponsive during all four FWD tests; the bottom gauge did not function in December. During grading of the berm at Section 5, the wires to all instrumentation were severed. Wires were spliced back together and testing was performed with satisfactory results. The top Dynatest gauge failed in the January test. In Section 6, the top HBM gauge was lost during installation. The encapsulated strain gauge was rendered inoperative from hot asphalt concrete burning through the wire. It was discovered that the protective coating on the connecting wire to the HBM gauges stopped just short of the gauge. This left a small end of wire unshielded. Subsequent installation of HBM gauges was performed successfully using heat resistant shrink tubing placed over the exposed wire.

### **3.3.2 Traffic Control**

Section 1 was unavailable for testing in April due to traffic control. Testing in Section 3 in January could not be conducted because of traffic control. Traffic control prohibited the closing of

Section 5 for testing in December and April. At Section 6, the four lane constructed highway narrowed to a two lane. With the inability to close the driving lane to traffic, only one FWD test (September) was conducted on this section.



## CHAPTER 4

### DATA ANALYSIS PROCEDURES

#### 4.1 SCOPE

After testing was completed, the field data required analysis and conditioning. Conditioning consisted of digital filtering of the data to eliminate unwanted noise, use of various calibration factors to convert the data into engineering units, and the use of mathematical algorithms to obtain characteristics of pavement responses (such as stresses). Data from each type of gauge used in the FWD testing required individual processing and analysis, as well as the data from the instrumentation used to collect environmental data.

#### 4.2 FWD TESTING

Raw data was recorded and stored on the EGAA system in binary format during FWD testing. The data files were downloaded off the EGAA system, converted into ASCII form, and filtered, before analysis commenced. The converted data was then loaded into an engineering spreadsheet and graphical software package for further processing.

The following sections explain the analysis procedure for each type of gauge used for FWD testing in more explicit detail.

##### 4.2.1 Strain Gauge Pressure Cells

The signal output from the pressure cells contained only a marginal level of noise. The data was downloaded directly without the use of the low pass filter. The data was then set to a zero baseline by subtracting the first data point from all the subsequent data points. The signal, measured

in volts, was then converted to a pressure using the calibration factor for psi/volts. The result was the pressure measured in psi at pavement/base and base/sub-grade interfaces.

#### 4.2.2 Dynatest Strain Gauge

Inspection of the data collected from the PAST-IIAC strain gauges revealed noise in the signal at a range of 60 Hz. The noise was due probably to the power source or computer boards. A finite impulse response, low pass digital filter program that used a Kaiser-Window was developed by personnel at the CGER to remove signal noises. The filter program converted the signal to an energy spectrum in the frequency domain. It then removed any signal above a selected frequency. The program then changed the signal back into the time domain and converted it to ASCII format. The selected frequency was 55 Hertz, since the noise centered at 60 Hertz. After several trials, it was determined that the filter could run at a frequency of 55 Hertz without distorting data peaks.

From measured voltage reading, strain values were calculated in accordance with the resistance change of a Wheatstone Bridge, as shown:

$$\Delta V_M = V_B \frac{R_1 R_2}{(R_1 + R_2)^2} \left( \frac{\Delta R_1}{R_1} - \frac{\Delta R_2}{R_2} + \frac{\Delta R_3}{R_3} - \frac{\Delta R_4}{R_4} \right) \quad 4.1$$

where  $\Delta V_M$  = Measured Voltage Change (volts)

$V_B$  = Bridge Voltage (volts)

$R_1$  = Strain Gauge Resistance (ohms)

$R_2 = R_3 = R_4$  = Internal Resistance (ohms)

The last three terms in Equation 4.1 can then be set equal to zero because the internal resistance of the bridge completion circuit does not change. This yields:

$$\Delta V_M = V_B \frac{R_1 R_2}{(R_1 + R_2)^2} \left( \frac{\Delta R_1}{R_1} \right) \quad 4.2$$

the resistance across the gauge relates to strain according to:

$$\frac{\Delta R_1}{R_1} = S_g \epsilon \quad 4.3$$

where  $\epsilon$  = Strain

$S_g$  - Strain Gauge Factor

R = Resistance

Combining Equations 4.2 and 4.3 and dividing by the gain set on the amplifiers yields:

$$\epsilon = \frac{\Delta V_M}{V_B} \frac{(R_1 + R_2)^2}{R_1 R_2} \frac{1}{S_g G} \quad 4.4$$

where  $\epsilon$  = Strain (micro-strains)

$\Delta V_M$  = Measured Voltage Change (volts)

$V_B$  = Bridge Voltage (volts)

G = Gain Factor

$S_g$  = Strain Gauge Factor

$R_1$  = Strain Gauge Resistance (ohms)

$R_2$  = Resistance of Completion Resistance (ohms)

Since  $R_1$  and  $R_2$  are the same, 120 ohm, Equation 4.4 can be further reduced to Equation 4.5 which was used in the conversion of the filtered data to a strain measurement.

$$\epsilon = \frac{\Delta V_M * 4}{S_g * G * V_B} \quad 4.5$$

Once the data was converted to strain, it was then represented graphically. In order to calculate the stresses in the pavement, the measured strain values were multiplied by the appropriate modulus of elasticity for the pavement. The variation of the modulus with respect to temperature required that values for each specific test were needed. The required conversion was based on the

graph taken from Kelly (9) as shown in Figure 4.1. Using measured temperature values at each test site, the modulus of the asphalt concrete was determined.

#### 4.2.3 HBM Encapsulated Strain Gauge

FWD data, collected using the HBM DA 3 encapsulated strain gauge, closely resembled that of the Dynatest gauges. Noise, located at 60 Hertz, was present and required the use of the low pass filter to remove. Conversion of the filtered data from the HBM gauges into strain values was achieved using Equation 4.4. The only difference was the change of strain gauge resistance from 120 ohms to 350 ohms. This had no influence since Equation 4.4 further reduces to Equation 4.5 regardless of the values for  $R_1$  and  $R_2$  (as long as they are equal).

#### 4.2.4 Accelerometers

The data signal collected in the field measured the acceleration of the pavement during FWD testing. The analysis of the data required the conversion from an acceleration to a deflection. This was accomplished by integrating the signal twice. The double integration analysis of the accelerometer data was performed using a program developed by personnel at CGER. The program converted the data into a voltage using Equation 4.6.

$$Voltage = Data * \left( \frac{20V}{4096} \right) \quad 4.6$$

The 20V factor is due to the +/- 10 V range of the gauge. The value of 4096 is 12 bit resolution used by the computer. The voltage was then converted into an acceleration (g) by adjusting for the sensitivity of the gauge. The signal was then integrated to calculate velocity. This was accomplished by summing data points collected during the time interval (1 second) that the sample was taken. This method of "integration" was sufficiently accurate because the sampling rate was

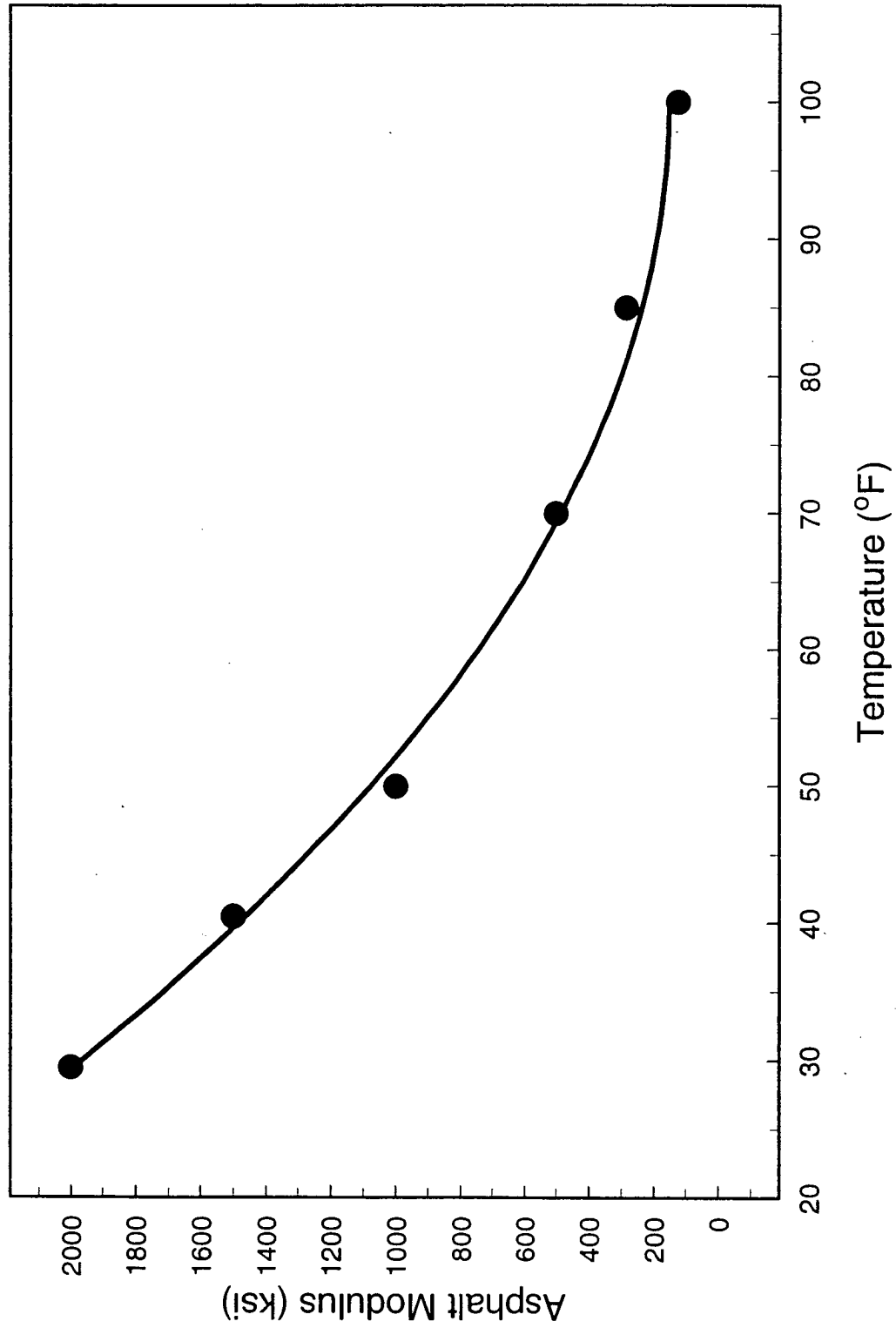


Figure 4.1 Variation of Asphalt Modulus with Temperature

much higher than the highest frequencies in the signal. The velocity was then integrated in the same manner as the acceleration. The second integration returned the data as a deflection. The output was then converted into units usable for analysis of the pavement by:

$$\delta = \frac{g*12 (inch/ft)}{S^2} \quad 4.7$$

where  $\delta$  = Deflection (inches)  
g = Result of the two "integrations"  
S = Number Data Points (2000/sec.)

#### 4.2.5 LVDTs

The data were set to a zero baseline by subtracting the first data point from all the subsequent data points. The signal, measured in volts, was then converted to a displacement using the calibration factors in volts/inch. The resultant was the deflection of the pavement due to the falling weight deflectometer measured in inches.

### 4.3 ENVIRONMENTAL DATA

The collection of environmental data was performed for each section during FWD testing. Data used to obtain the moisture content of the base and subgrade were collected along with temperature readings at the top and bottom of the asphalt concrete, as well as the center of the base layer.

#### 4.3.1 Soil Moisture Probes

The system, developed by Campbell Scientific based on TDR, measures the velocity of a waveform as it propagates down a waveguide. The signal output from the probes, received by the datalogger, was converted to volumetric water content using Ledieu's calibration, as shown:

$$W_v = \left( \frac{0.1138}{V_p} \right) * 0.1758 \quad 4.8$$

where  $W_v$  = Volumetric Water Content  
 $V_p$  = Waveform Propagation Velocity

The volumetric water content was related to soil moisture content in terms of mass according to:

$$W_v = W_m * G \quad 4.9$$

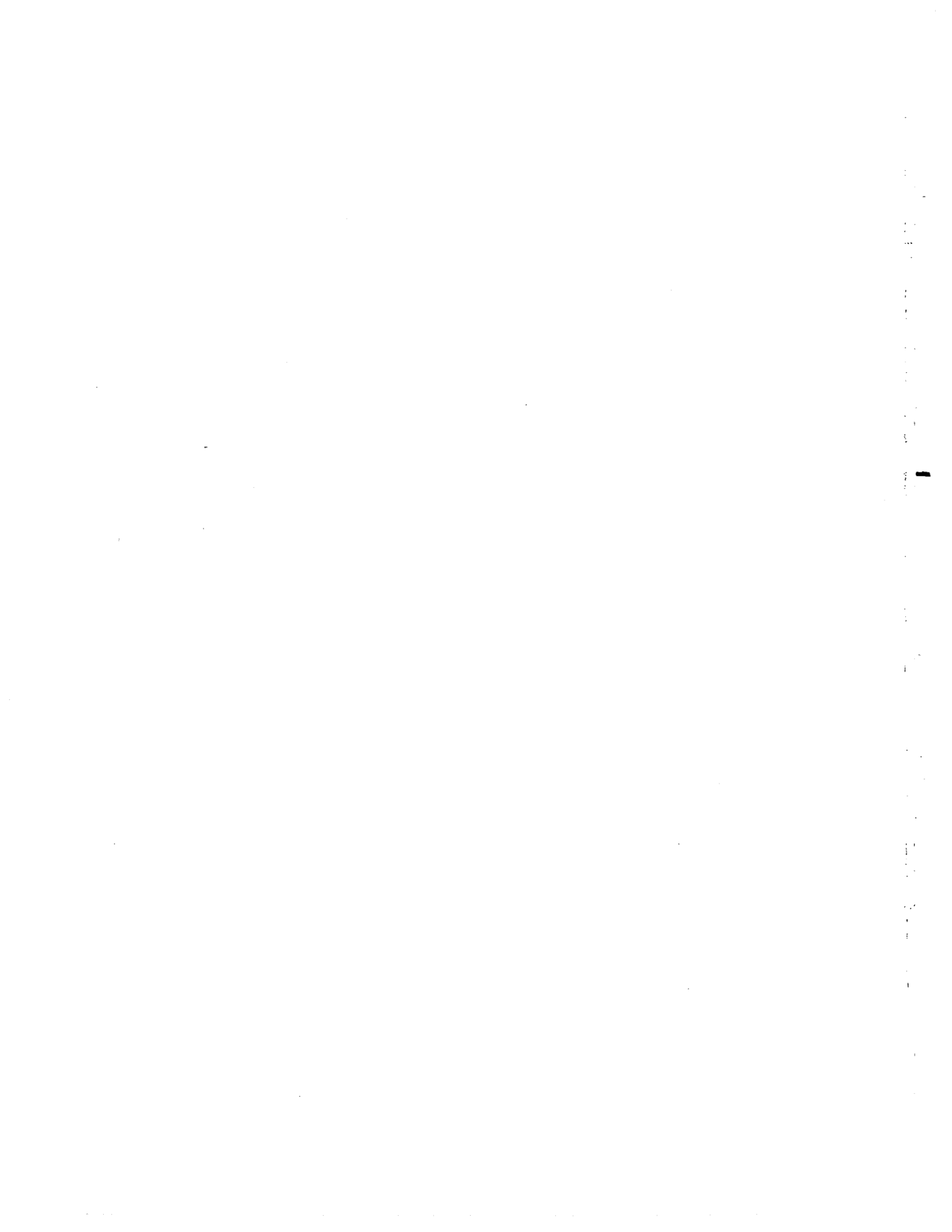
where  $G$  = Specific Gravity of the Soil  
 $W_m$  = Soil Moisture Content  
 $W_v$  = Volumetric Water Content

Using measured volumetric water content and the specific gravity provided by ODOT personnel, the soil moisture content was calculated using:

$$W_m = \frac{W_v}{\gamma_s} \quad 4.10$$

where  $\gamma_s$  = Unit Mass of Soil

The unit weights taken were 2.33 grams/cm<sup>3</sup> for the 304 base material and 1.81 grams/cm<sup>3</sup> for the subgrade.



## CHAPTER 5

### ENVIRONMENTAL AND FWD DATA RESULTS

#### 5.1 INTRODUCTION

Results discussed in this chapter are from four separate FWD tests. Deflection, pressure, and strain results are listed corresponding to each section and the respective season when the test was conducted. Each of the gauge responses shows the influence of the impulse load on the asphalt concrete in correspondence with the environmental conditions at the time of testing.

#### 5.2 DISCUSSION OF ENVIRONMENTAL MEASUREMENTS

Table 5.1 displays the environmental conditions of moisture and temperature for each of the sections during each test. This includes the soil moisture content in the base and subgrade, as well as the temperature in the base and the top and bottom layers of asphalt concrete. Moisture content in the subgrade and base stayed fairly constant in Sections 1 and 2 during the FWD tests. However, the moisture in the remaining sections varied with seasons. It was not anticipated since the asphalt concrete was newly placed and no cracking was observed. Water would drain off the pavement with little to no infiltration, thus maintaining the moisture content the same throughout the seasons tested. This was true for Sections 1 and 2, but for Sections 3,4,5, and 6, moisture levels changed. Moisture levels appear to correspond to elevation of sections. Elevations of Sections: Section 1 - 1461; Section 2 - 1411; Section 3 - 1320; Section 4 - 1410; Section 5 - 1166; and, Section 6 - 1165. The two-foot-deflection measures the pavement and base deformation under the application of FWD loading. As expected, Section 2 measures the least deflection and lowest moisture among the

Table 5.1 Environmental Data for Asphalt Concrete

Environmental Data						
Month tested	Section	Soil Moisture Probe	Volumetric Moisture Content (%)	Weight Moisture Content (%)	Thermocouple	Temp. (°F)
December 1993	1	SM-01	14.7	8.1	TC-01	34
		SM-02	22.3	9.6	TC-02	32
	2	SM-01	32.2	17.8	TC-01	33
		SM-02	17.9	7.7	TC-02	33
April 1994	3	SM-01	23.9	13.2	TC-03	34
		SM-02	21.7	9.3	TC-01	35
	4	SM-01	23.3	12.9	TC-02	32
		SM-02	34.9	15.0	TC-03	34
September 1994	2	SM-01	32.5	18.0	TC-01	63
		SM-02	16.1	6.9	TC-02	66
	3	SM-01	*	*	TC-03	71
SM-02		*	*	TC-01	63	
September 1994	4	SM-01	31.7	17.5	TC-02	67
		SM-02	28.4	12.2	TC-03	75
September 1994	1	SM-01	15.2	8.4	TC-01	65
		SM-02	16.8	7.2	TC-02	62
September 1994	2	SM-01	31.9	17.6	TC-03	63
		SM-02	16.8	7.2	TC-01	65
September 1994	2	SM-01	31.9	17.6	TC-02	63
		SM-02	16.8	7.2	TC-03	64

Table 5.1 Environmental Data for Asphalt Concrete (continued)

Environmental Data						
Month tested	Section	Soil Moisture Probe	Volumetric Moisture Content (%)	Weight Moisture Content (%)	Thermocouple	Temp. (°F)
September 1994 (con't.)	3	SM-01	40.4	22.3	TC-01	68
		SM-02	22.9	9.8	TC-02 TC-03	66 68
	4	SM-01	40.4	22.3	TC-01	68
		SM-02	22.9	9.8	TC-02 TC-03	69 71
5	SM-01	42.8	23.6	TC-01	69	
	SM-02	41.9	18.0	TC-02 TC-03	70 73	
6	SM-01	30.7	17.0	TC-01	68	
	SM-02	26.6	11.4	TC-02 TC-03	70 73	
January 1995	1	SM-01	15.0	8.3	TC-01	33
		SM-02	31.9	13.7	TC-02 TC-03	37 37
		SM-01	31.4	17.4	TC-01	35
	2	SM-02	16.5	7.1	TC-02 TC-03	35 37
		3	SM-01	29.8	16.5	TC-01
SM-02	28.2		12.1	TC-02 TC-03	37 38	
4	SM-01	29.8	16.5	TC-01	35	
	SM-02	28.2	12.1	TC-02 TC-03	37 38	
5	SM-01	32.9	18.2	TC-01	36	
	SM-02	41.5	17.8	TC-02 TC-03	37 38	

sections tested. Moisture content remains between 7.4 and 15% by weight except for Section 5 (crushed 304 base) where the moisture is 17.6%. Two-foot-deflections appear to be related to seasonal change and type of base rather than moisture content. Moisture in the subgrade for Section

1 and 2 were constant. Total pavement deflection appears related to season and type of pavement rather than moisture. Also, there appears to be no correlation between moisture present and pressures on base and subgrade.

Larger pavement deflections, pressures, and strains were measured in the warmer months of April and September, as expected, rather than during tests conducted in December and January. During the tests, the temperature profile was uniform. In the spring (April) the temperature at the surface of the asphalt concrete was warmer than the bottom of the asphalt concrete. In Section 4, the difference was 13°F. (This is discussed in the next section.) Temperature was the most significant factor affecting deflections, pressures, and strains measured for flexible pavement. The modulus of asphalt concrete changes significantly with temperature. Figure 4.1 shows a graph of modulus of asphalt concrete with respect to temperature. In the temperature range for the tests conducted, the modulus of the asphalt concrete varied from 200 ksi in April to 1800 ksi in December. In addition, temperatures of 32°F measured at the pavement/base interface indicated that there may have been some frozen material present during the December tests.

### **5.3 DATA ANALYSIS FOR FWD**

The analysis of FWD data includes deflection, pressure, and strain readings for each section. Numerical results are tabulated for all sections for each test period. The following summarizes the discussion for this section:

- A comparison of deflections for the ten foot anchor, accelerometer, and geophone are presented, along with pavement temperature.
- Deflections measured for rods anchored at reference depths of ten, six, four, and two feet are tabulated. (The reference depth of ten feet gives the best comparison with accelerometer and

geophone measurements. The two foot anchored rod gives an indication of deflection occurring in the pavement and base.)

- Temperatures, and pressures, monitored at the pavement/base and base/subgrade interfaces, are presented.
- The maximum values of strain are recorded.

All mechanical response amplitudes were read from time response to an impact load. A comparison of sections is made later in the chapter.

### **5.3.1 Deflection Measurements Under FWD Loading**

Table 5.2 presents a comparison of the deflections obtained from accelerometer, geophone, and LVDT. Figure 5.1 illustrates the close agreement obtained from the accelerometer signal response when compared to the movement of a rod anchored at the ten foot depth. Testing of Section 1 during several seasonal weather conditions provided significantly different measurements. As shown in Table 5.2, a deflection measured by the accelerometer during the cold weather month of December was 4.56 milli-inches. The accelerometer measurements in January produced a 5.38 milli-inch deflection. These measurements contrast with the deflection value measured in August of 16.27 milli-inches. Since the moisture in subgrade stayed constant, this large change in deflection can be attributed to the large change in modulus of base.

Section 2 underwent the least deflection in all the seasonal tests. Deflections were larger in the warmer months than in the colder months, but the differences were not as large as for the ATB sections (Section 1). As shown in Table 5.2, the accelerometers measured deflections of 9.28 and 9.88 milli-inches during the April and September tests, respectively. These readings were larger than the 3.14 and 4.61 milli-inches measured during the December and January tests. Measurements

Table 5.2 Comparison of Pavement Deflections when Loaded with FWD

FWD Deflection Data									
Month tested	Section	Load (lb)	Accelerometer (E-6 in)	Geophone (E-6 in)	Load (lb)	10 ft. LVDT (E-6 in)	Geophone (E-6 in)	Temperature (°F)	
December	1	14216	4.56	6.28	14428	4.9	6.91	36	
	2	14088	3.14	3.98	15168	3.8	4.79	35	
	3	15328	3.9	4.27	--	--	--	33	
	4	15352	4.67	5.91	16160	5.2	6.36	32	
April	2	15950	9.28	9.04	16414	7.5	11.63	68	
	3	14984	7.93	8.93	--	--	--	71	
	4	--	--	--	--	13	14.04	--	
	1	17128	16.27	18.43	16568 & 17000	10 & 9.8	21.85 & 12.39	84 & 63	
August and September	2	15748	9.88	10.94	16368	8 & 5.3	6.62	88 & 64	
	3	15520	9.34	9.78	16976	12	6.32	87 & 68	
	4	15016	12.43	14.81	16016	13 & 7.5	9.38	91 & 64	
	5	15128	15.29	16.58	16208	18 & 9.5	11.71	90 & 73	
	1	17097	5.38	6.22	17638	4	5.9	37	
January	2	17447	4.61	4.8	16500	3.5	5.4	37	
	3	--	--	--	--	2.5	3.9	--	
	4	18130	3.69	3.74	17638	1.4	3.7	38	
	5	17240	4.62	4.64	17095	3.6	5.4	38	

SECTION 1 PAVEMENT RESPONSE  
DECEMBER FALLING WEIGHT DEFLECTOMETER TEST

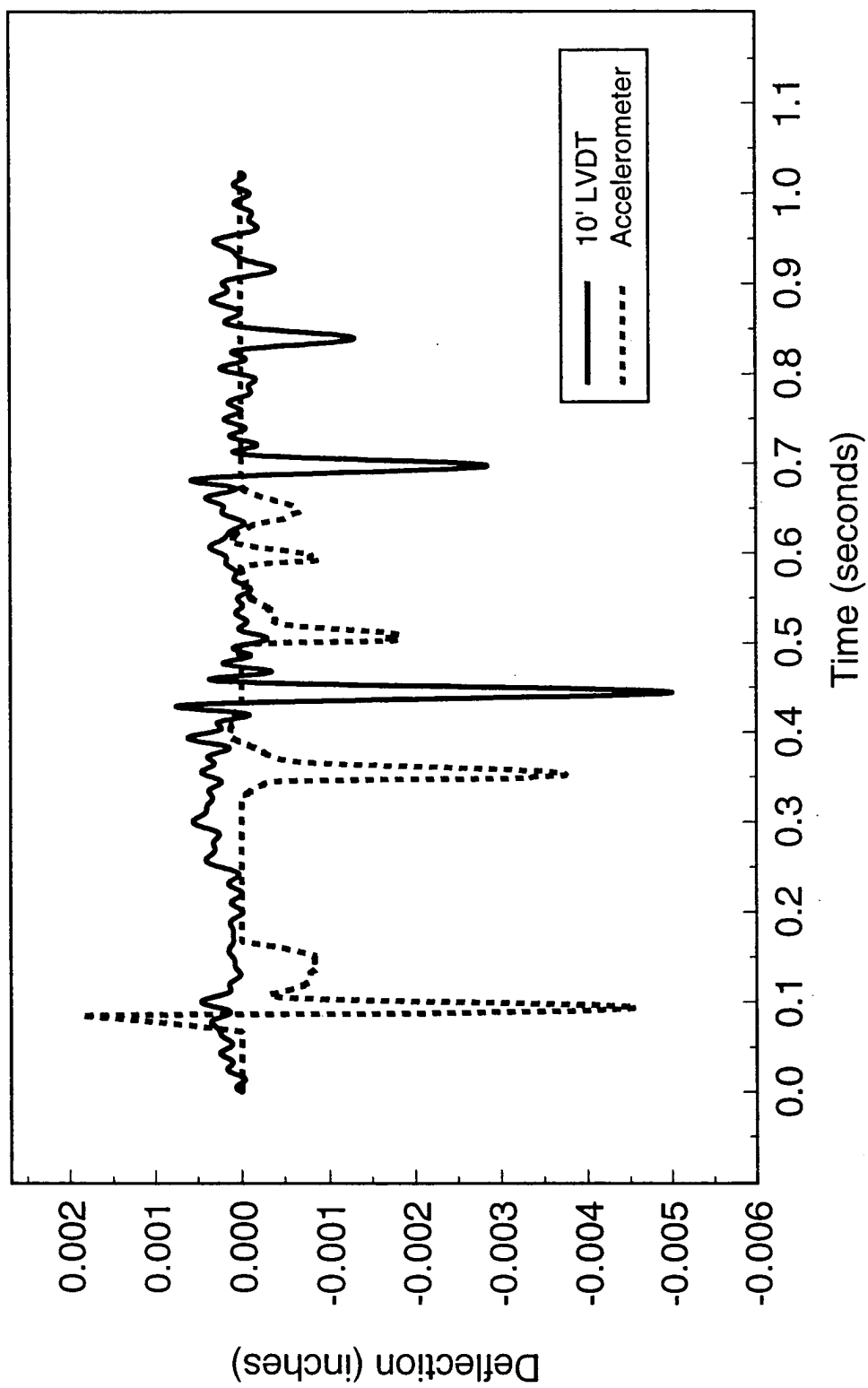


Figure 5.1 Comparison of Accelerometer and LVDT Deflection

taken during cold and warm weather yielded values for the accelerometer that paralleled values from the LVDT and geophone. Deflections from December and January were consistent with each other with the exception of differences in the applied load. A deflection measured by the accelerometer of 3.14 milli-inches in December with a load of 14,088 lb. compares to 3.98 milli-inches read by the geophone in Section 2. The LVDT read 3.8 milli-inches during the same test with a load of 15,168 lb., respectively. The distribution of pavement deflections can be determined since LVDTs were anchored at depths of 2, 6, and 10 ft. Examining data (Table 5.3) for reference rods anchored at 2 ft. and comparing to geophone measurements for September, the percent of total deflection localized to the top are Section 1 - 82%; Section 2 - 36%; Section 3 - 46%; Section 4 - 66%; Section 5 - 64%; and, Section 6 - 64%.

The pattern of SLD (LVDT) deflections are the same for both the summer and winter. (See Table 5.3.) Typical results are shown in Figures 5.2 and 5.3, where Figure 5.2 shows the time response record for the December test, and Figure 5.3 shows the time response record for the April test. Most of the deflection, with respect to depth, appear to be in the subgrade for the PCTB Section (Section 2) Examining the SLD readings, the six-foot deflection is about 90% of the ten-foot deflection, whereas, the two-foot reading is only 25% of the ten-foot deflection.

As shown in Table 5.2 for Section 3, accelerometer deflection readings were approximately the same as for PCTB (Section 2). Testing performed in December yielded the smallest deflection, measured at 3.9 milli-inches. Testing during the warmer months of April and August produced larger deflections than December, with August being the largest at 9.34 milli-inches, followed by April at 7.93 milli-inches.

Table 5.3 Deflections for Single Level Deflectometers from FWD Tests

FWD Thickness Deflection Data				
Month Tested	Drop Location	Reference Depth (ft.)	Measured Deflection (E-6 in)	
			LVDT	Geophone
December	S1LVDT1	10	4.9	6.91
	S1LVDT2	6	5.6	6.84
	S1LVDT3	4	4.4	6.32
	S1LVDT4	2	4.1	6.4
	S2LVDT1	10	3.8	4.79
	S2LVDT2	6	3.6	4.31
	S2LVDT3	4	2.4	4.59
	S2LVDT4	2	1.4	4.18
	S4LVDT1	10	5.2	6.36
	S4LVDT2	6	5	7.24
	S4LVDT3	4	3.7	6.52
	S4LVDT4	2	2.8	6.64
April	S2LVDT1	10	7.5	11.63
	S2LVDT2	6	5.3	9.86
	S2LVDT3	4	6.4	10.46
	S2LVDT4	2	2.7	9.21
	S3LVDT2	6	7.4	9.98
	S3LVDT3	4	5.3	9.74
	S3LVDT4	2	4.8	9.38
	S4LVDT1	10	13	14.04
	S4LVDT2	6	8.5	15.4
	S4LVDT3	4	11	13.52
	S4LVDT4	2	7	12.84

Table 5.3 Deflections for Single Level Deflectometers from FWD Tests (continued)

Month Tested	Drop Location	Reference Depth (ft.)	Measured Deflection (E-6 in)	
			LVDT	Geophone
<i>August and September</i>	S1LVDT1	10	9.8	12.39
	S1LVDT2	6	8.9	12.51
	S1LVDT4	2	10.1	12.28
	S2LVDT1	10	8.0 & 5.3	6.62
	S2LVDT2	6	5.2	7.94
	S2LVDT4	2	2.6	7.28
	S3LVDT1	10	12	6.32
	S3LVDT2	6	9	6.56
	S3LVDT4	2	3	6.44
	S4LVDT1	10	13.0 & 7.5	9.38
	S4LVDT2	6	6.6	9.6
	S4LVDT4	2	6.4	9.61
	S5LVDT1	10	18.0 & 9.5	11.71
	S5LVDT2	6	8	11.15
	S5LVDT4	2	6	9.29
	S6LVDT2	6	5.9	7.21
	S6LVDT4	2	4.5	7.02
	January	S1LVDT1	10	4
S1LVDT2		6	3.9	5.6
S1LVDT3		4	3.3	5.5
S1LVDT4		2	2.7	5.4
S2LVDT1		10	3.5	5.4
S2LVDT2		6	2.8	5.5

Table 5.3 Deflections for Single Level Deflectometers from FWD Tests (continued)

Month Tested	Drop Location	Reference Depth (ft.)	Measured Deflection (E-6 in)	
			LVDT	Geophone
January (continued)	S2LVDT3	4	3	5.4
	S2LVDT4	2	1	5.4
	S3LVDT1	10	2.5	3.9
	S3LVDT2	6	1	3.9
	S3LVDT3	4	1.1	4
	S3LVDT4	2	1.2	3.9
	S4LVDT1	10	1.4	3.7
	S4LVDT2	6	1.5	3.2
	S4LVDT3	4	1.5	3.3
	S4LVDT4	2	1	3.8
	S5LVDT1	10	3.6	5.4
	S5LVDT2	6	3.1	5
	S5LVDT3	4	2.9	4.7
	S5LVDT4	2	2	4.6

SECTION 2 - LVDT Response  
Falling Weight Deflectometer December Test

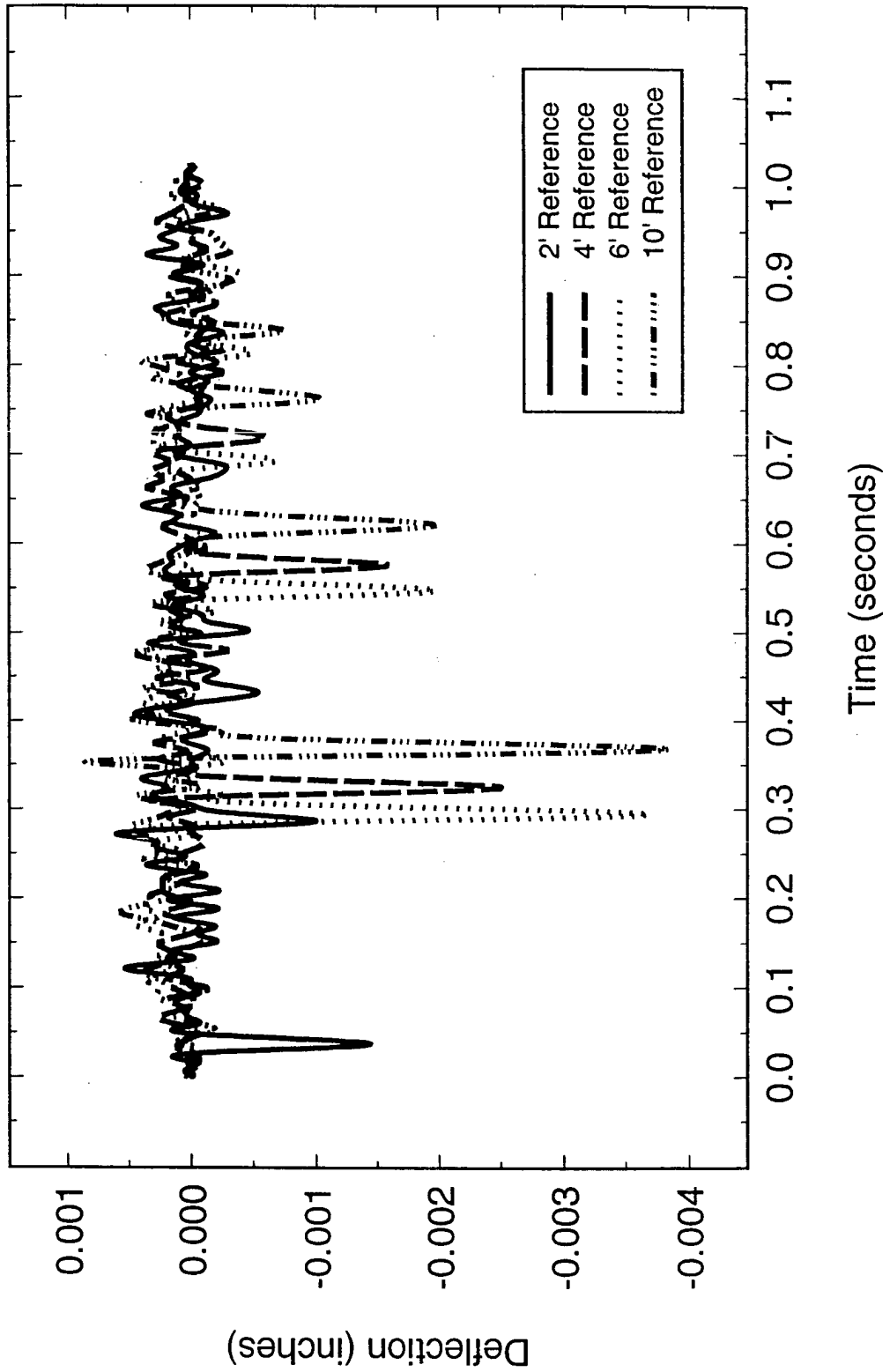


Figure 5.2 SLD Response from December FWD Test

SECTION 2 - LVDT Response  
 Falling Weight Deflectometer April Test

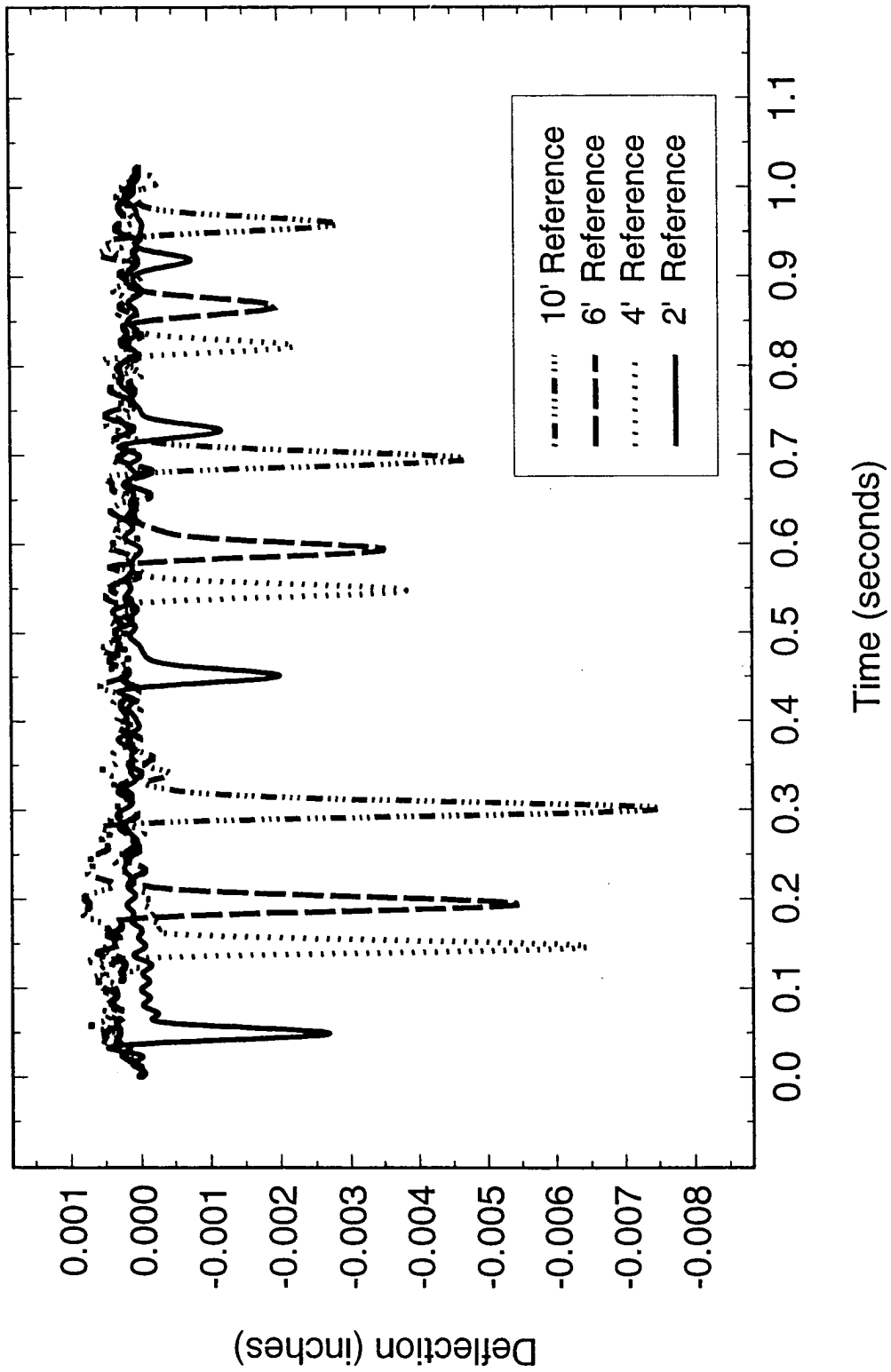


Figure 5.3 SLD Responses From April FWD Test

Accelerometer deflections of Section 4 were somewhat less than for the ATB (Section 1). The largest deflection of 12.43 milli-inches was recorded in April and the reading in January was 3.69 milli-inches.

Data were collected in September and January for Section 5. This data pertained to deflection of the pavement under warm and cold weather situations. Data collected for the two tests correlated with data recorded from the NJ site (Section 3) under similar environmental conditions. The LVDT deflection for the September test was 9.5 milli-inches, while in January the deflection was 3.6 milli-inches.

Only limited data was collected on Section 6. The deflection of the six foot SLD (Table 5.3) showed a deflection of 6.5 milli-inches in September.

Data were collected on all sections so that comparisons could be made. The total deflection of pavement surface is plotted versus the pavement temperature at time of testing in Figures 5.4 and 5.5. There is good agreement with SLD and geophone measurements. Examination of data shows that all test sections yield small deflections at low temperatures, due to the stiffness of asphalt concrete. However, the deflection of the PCTB (Section 2) and IA (Section 4) bases appear to provide the stiffer base.

In Figure 5.6, the average deflections are plotted versus Section number. Temperature varied with season. Magnitude of loads applied in tests are given in Table 5.2. From this figure it is obvious that the largest variation of deflection with season occurs with ATB. And, the least variation of deflection with season (temperature) occurs with PCTB. The NJ and PCTB bases respond similarly.

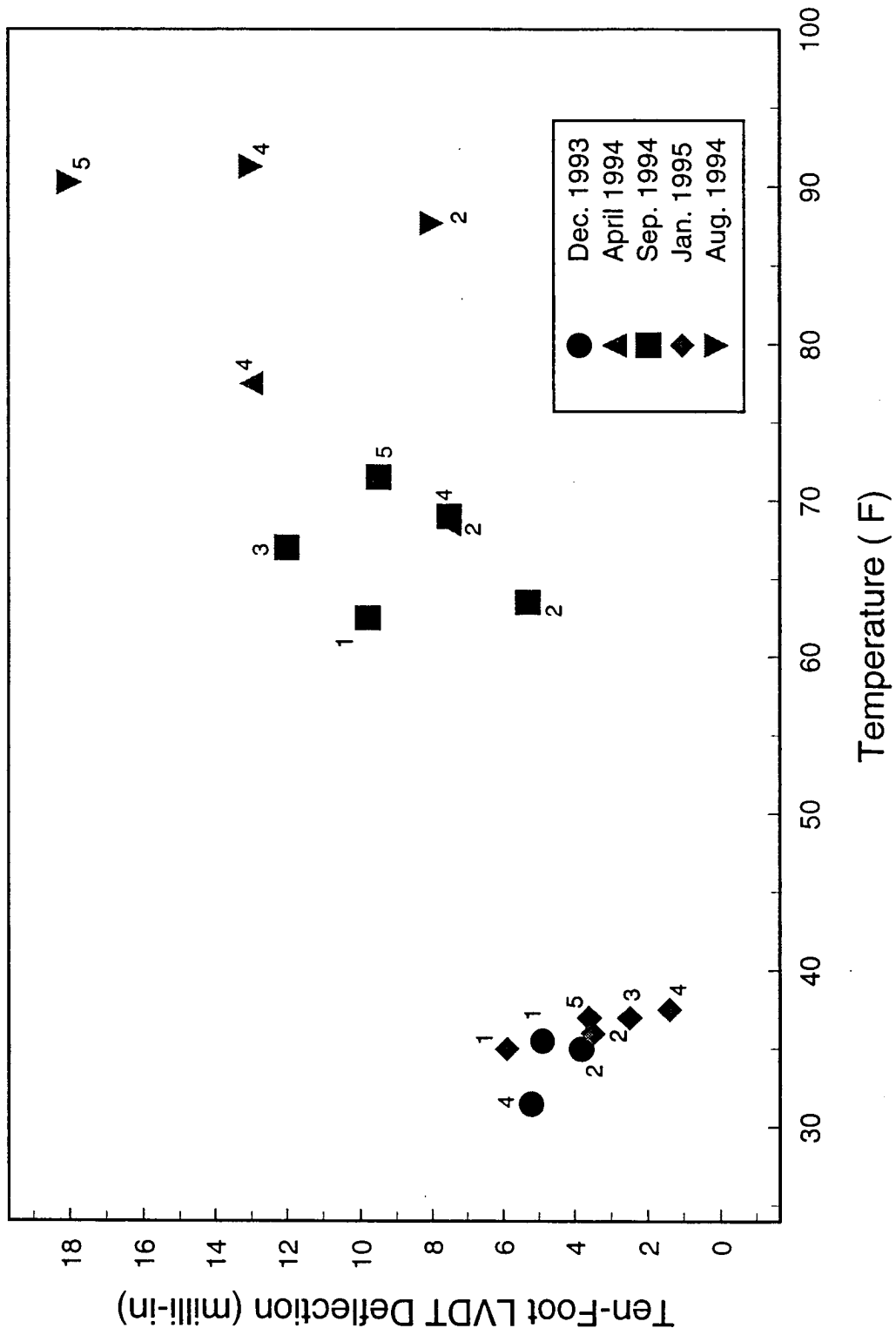


Figure 5.4 Pavement Deflection (SLD) Versus Pavement Temperature

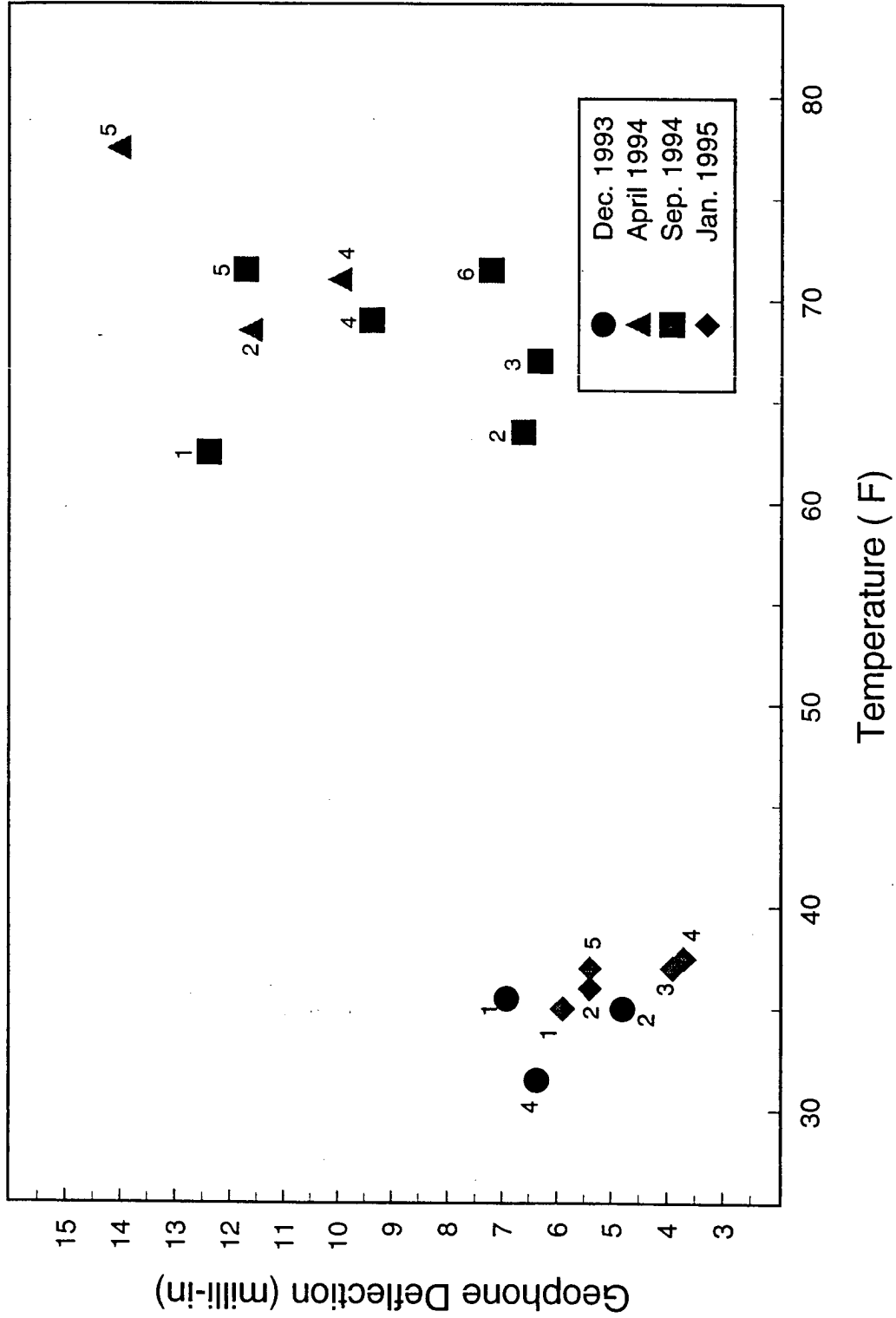


Figure 5.5 Pavement Deflection (Geophone) Versus Pavement Temperature

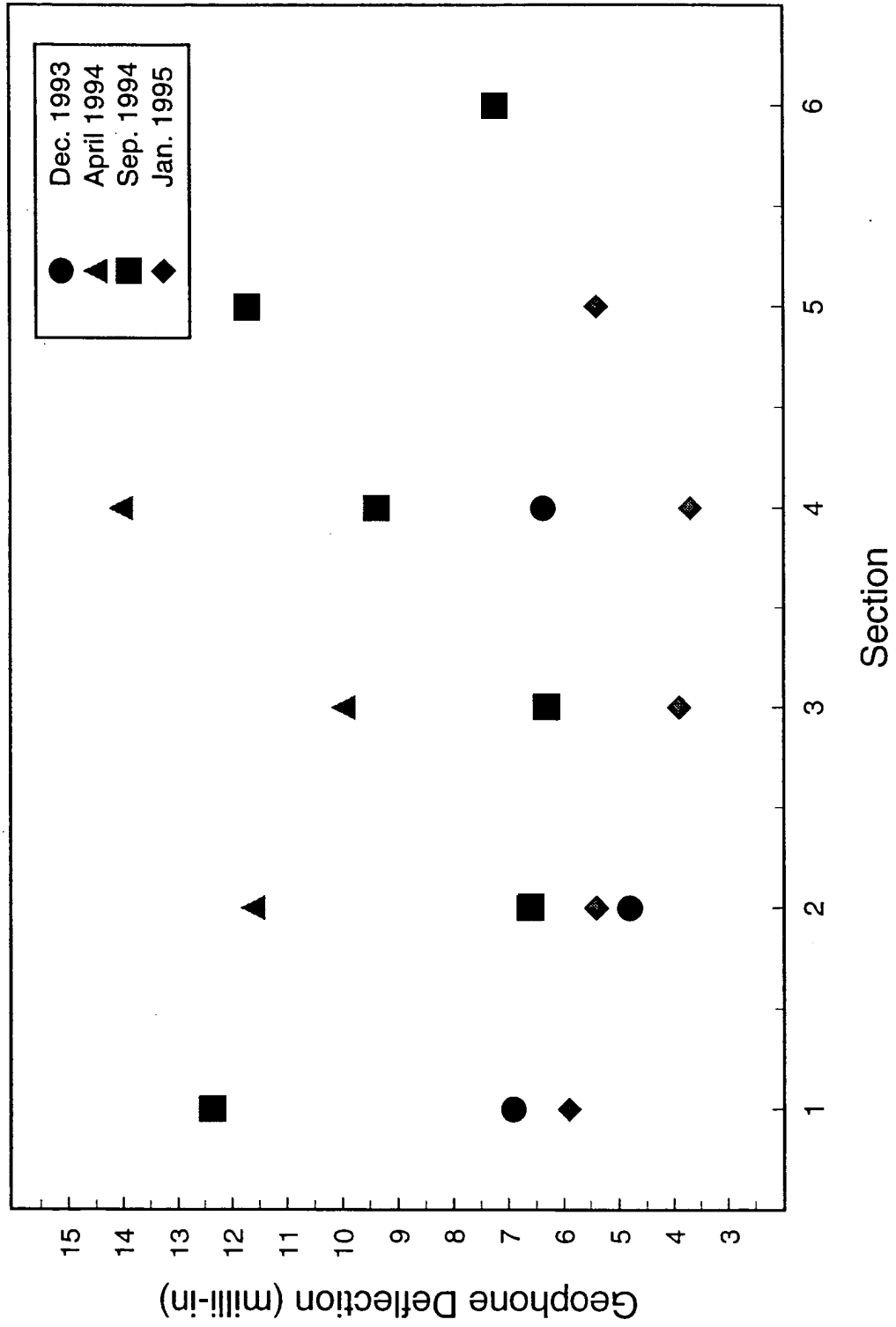


Figure 5.6 Pavement Deflection Versus Section Tested

To isolate the deflection that occurs in pavement and base layers, the deflection of the 2 foot reference rod can be examined in Figure 5.7. Here again, the ATB has the highest seasonal variation and the PCTB has the least seasonal variation. The NJ base appears to compare well with the PCTB.

### **5.3.2 Pressure Measurements Under FWD Loading**

Figure 5.8 shows the time response record of seasonal differences in pressure readings. Tests were conducted in December and September. Maximum values of all tests are recorded in Table 5.4. The pressure measurements reinforce the seasonal difference observed for deflection. December readings are approximately 60% less at the lower SGPC, whereas, in September, the difference in readings was only about 30%. Pressures recorded in December are 0.8 and 2.6 psi at the base/subgrade and asphalt concrete/base interfaces, respectively. During January, values were 0.6 and 2.9 psi. Larger pressures of 3.4 and 4.7 psi, consistent with warmer weather conditions, were observed in September at the bottom and top.

Again for Section 3, the pressure cell readings were smallest in December and January. Testing in December produced pressure values of 0.2 and 0.7 psi at the bottom and top of the base. Similarly, January measurements were 0.9 and 1.1 psi, respectively. Pressure values recorded during warmer weather testing were significantly larger. Values of 4.1 and 6.5 psi were measured in April. Likewise, under similar conditions, pressures of 4.5 and 5.3 psi were recorded in September.

In Section 4, the strain gauge, pressure cell responses were very similar to those in Section 2. The obvious difference, however, occurred for the large responses of the bottom pressure cells during April and September. The readings of 9.6 and 8.6 psi for these tests were much larger than the readings of 0.5 and 0.6 psi.

Pressure cell readings were logged in September and January for Section 5. In September,

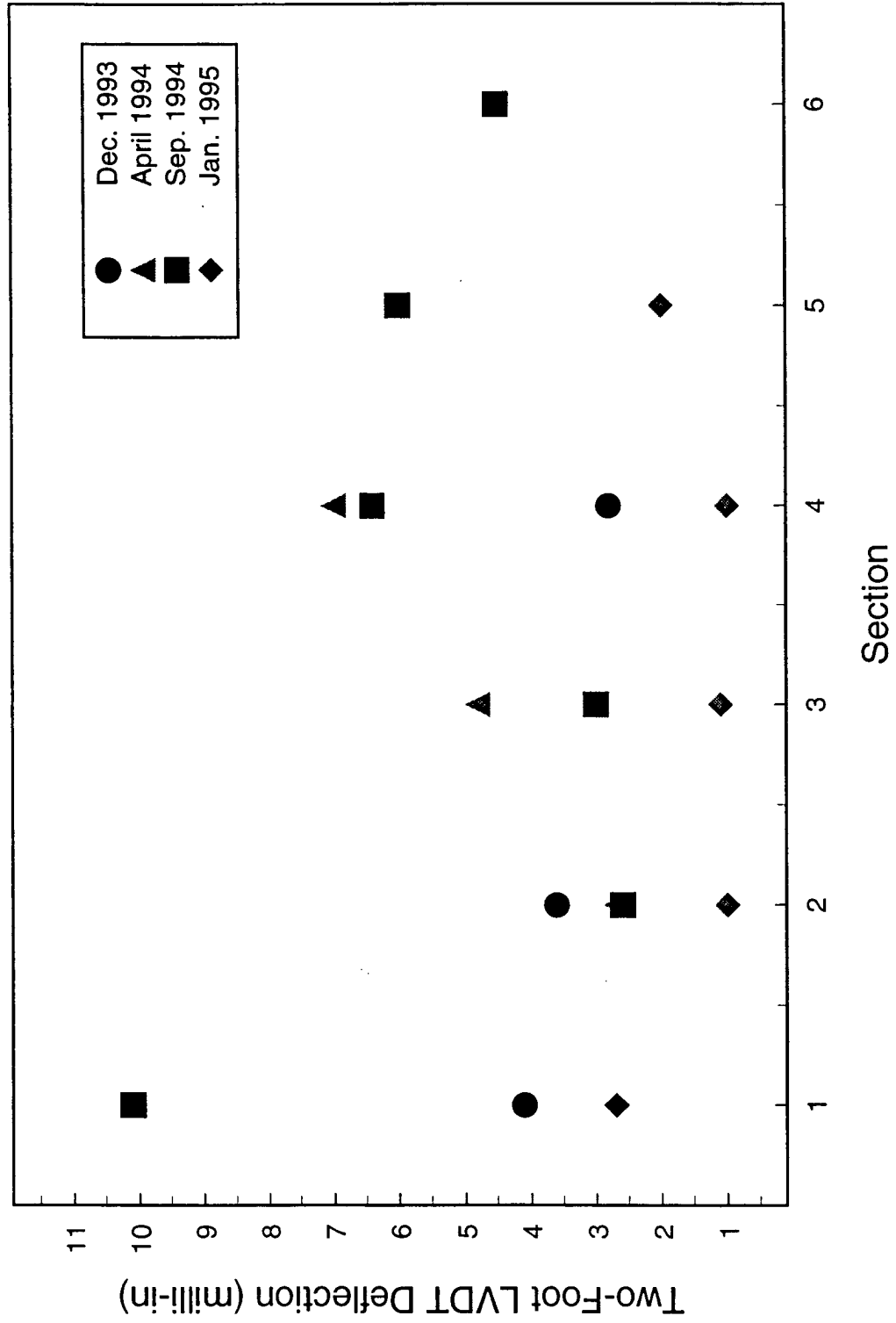


Figure 5.7 Pavement Deflection and Base Deformation Versus Section Tested

# SECTION 1 STRAIN GAUGE PRESSURE CELL RESPONSE

December and September Falling Weight Deflectometer Tests

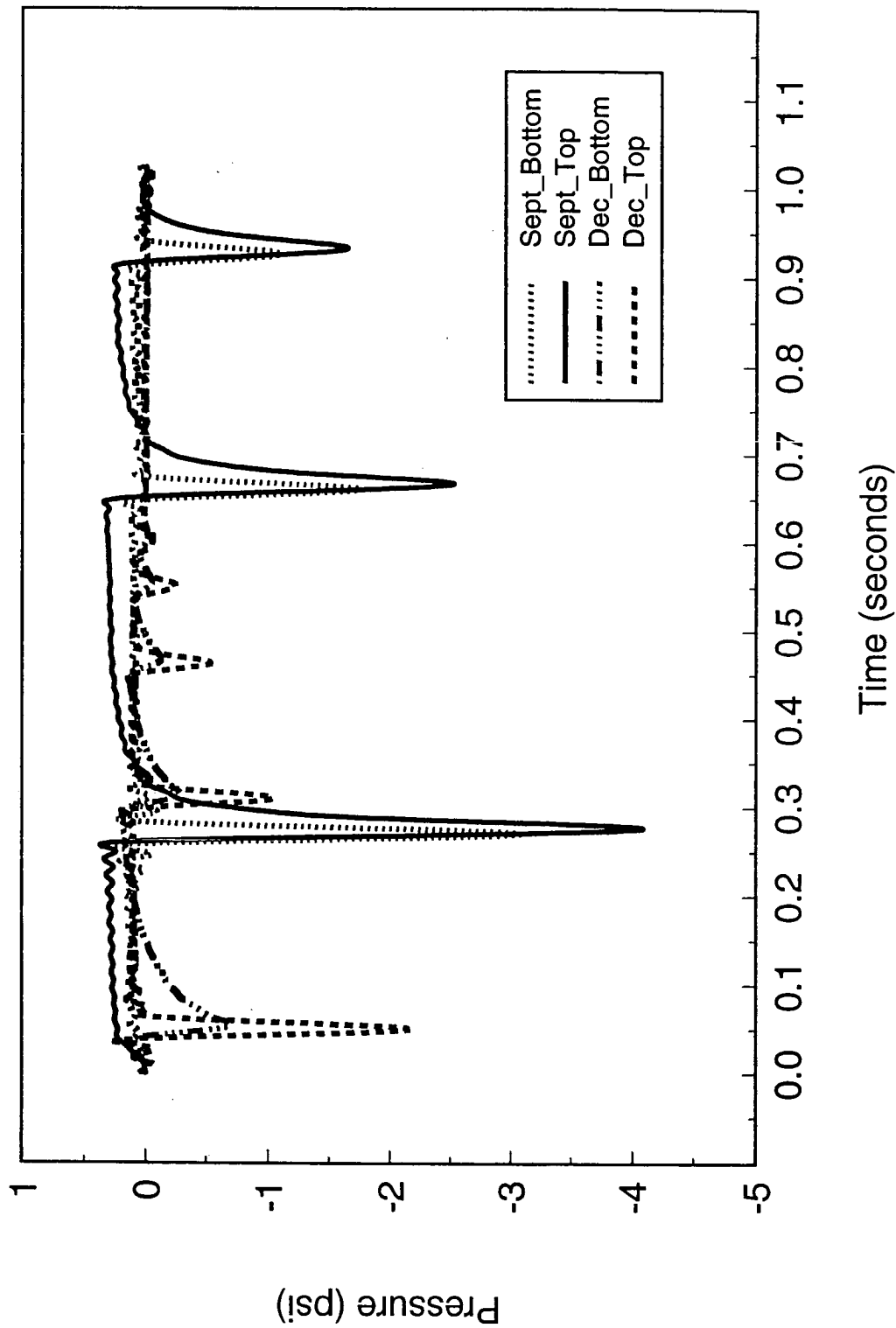


Figure 5.8: Time Response of Pressure Cells Subjected to FWD Loading

Table 5.4 Pressure Cell Data for FWD Loading

Month Tested	Section	Load (lb)	Pavement Temperature (°F)	Pressure Cells Monitored	Pressure (psi)
December	1	14440	39	SGPC01 SGPC02	0.8 2.6
	2	14336	37	SGPC01 SGPC02	0.5 0.8
	3	15768	34	SGPC01 SGPC02	0.2 0.7
	4	15512	32	SGPC01	0.6
April	2	15648	71	SGPC01 SGPC02	0.5 12.7
	3	15050	75	SGPC01 SGPC02	4.1 6.5
	4	15400	84	SGPC01 SGPC02	9.6 10.6
September	1	16115	63	SGPC01 SGPC02	3.4 4.7
	2	16272	64	SGPC01 SGPC02	0.6 5.5
	3	16176	68	SGPC01 SGPC02	4.5 5.3
	4	16056	71	SGPC01 SGPC02	8.6 12.1
	5	15832	73	SGPC01 SGPC02	2.8 8.0
	6	15840	73	SGPC01 SGPC02	4.3 6.7
January	1	17050	37	SGPC01 SGPC02	0.6 2.9
	2	17415	37	SGPC01 SGPC02	0.6 1.1
	3	17745	38	SGPC01 SGPC02	0.9 1.1
	4	18257	38	SGPC01 SGPC02	2.0 3.5
	5	17304	38	SGPC01 SGPC02	0.3 2.0

readings of 2.8 and 8.0 psi were recorded for the top and bottom of the base. In January, values of 0.3 and 2.0 psi were measured. Pressure cell readings for Section 6 were 4.3 psi for the bottom cell and 6.7 psi for the top cell in September, which are similar to the readings of Section 5.

Since there was only one test conducted on Section 6, comparisons cannot be made with other sections. Some of the readings for December and April may be larger because the final 1-1/4 inch asphalt concrete layer was not placed until after the April test.

Pressure readings were consistent with deflection measurements with larger values observed during April and September. For cold weather tests, the load was distributed throughout the pavement and base better due to the stiffer modulus of the material. There was a concern that inaccurate pressure cell readings would result from the contact of large aggregate with the sensitive face of the pressure cell at the interface between asphalt concrete and base because of the uneven pressure distribution, or that a gap could form between the asphalt concrete and the pressure cell face again giving false readings. However, since all pressure cell readings were consistent and reasonable, the installation procedure was considered to be successful.

Pressures recorded for the FWD tests are shown in Figures 5.9 and 5.10. FWD testing in the warmer months yielded pavement/base pressures at Section 1 smaller than for the other sections. The Iowa base gave pressures of the largest magnitudes for the base/subgrade interface. PCTB showed high pressures at the pavement/base interface during April and September. FWD testing in December and January resulted in large pavement/base pressures at Section 1 when compared to other sections.

### **5.3.3 Strain Gauge Measurements Under FWD Loading**

Strain gauge data collected from all sections are shown in Table 5.5. In the December test

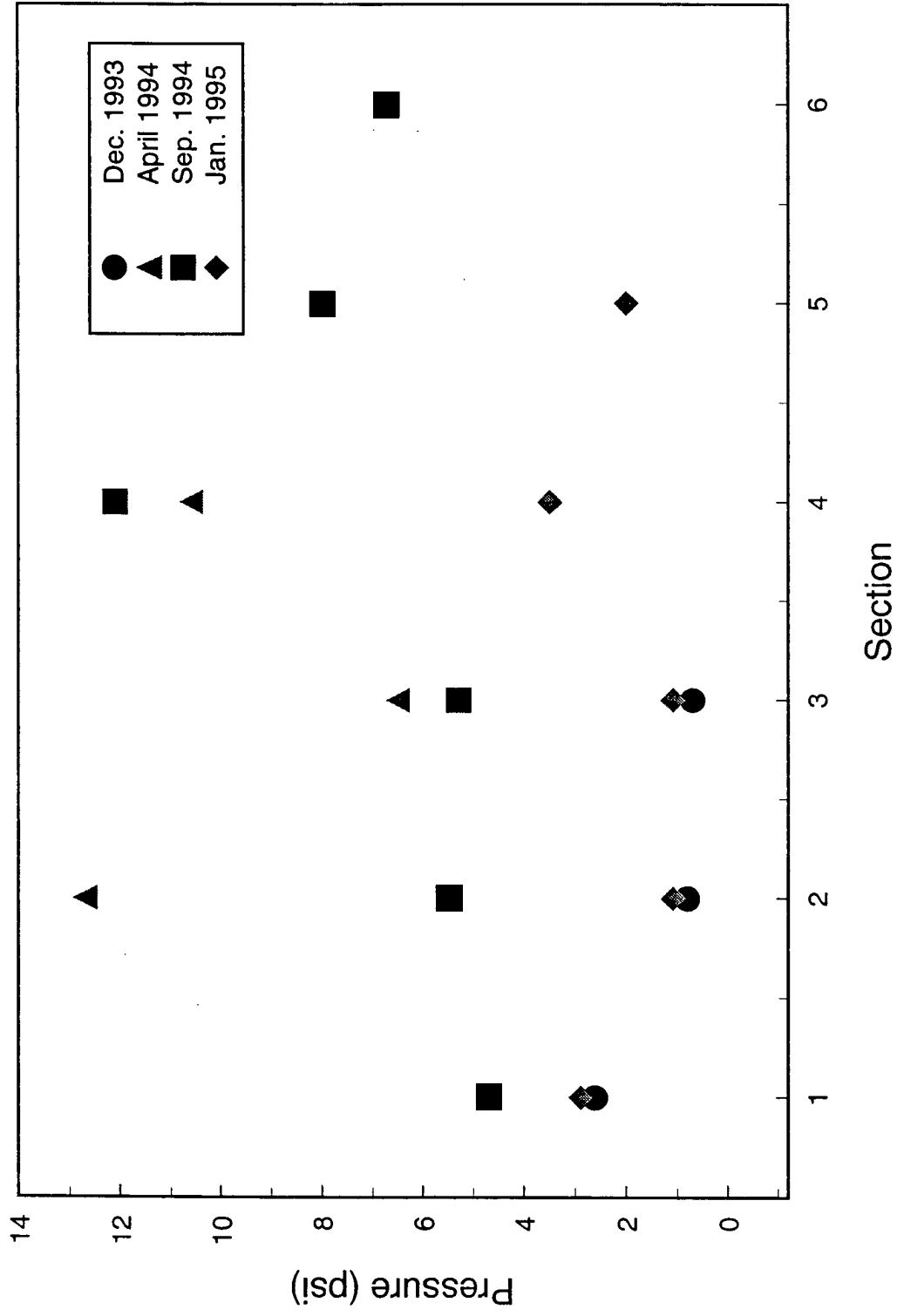


Figure 5.9 Base Pressures Versus Section

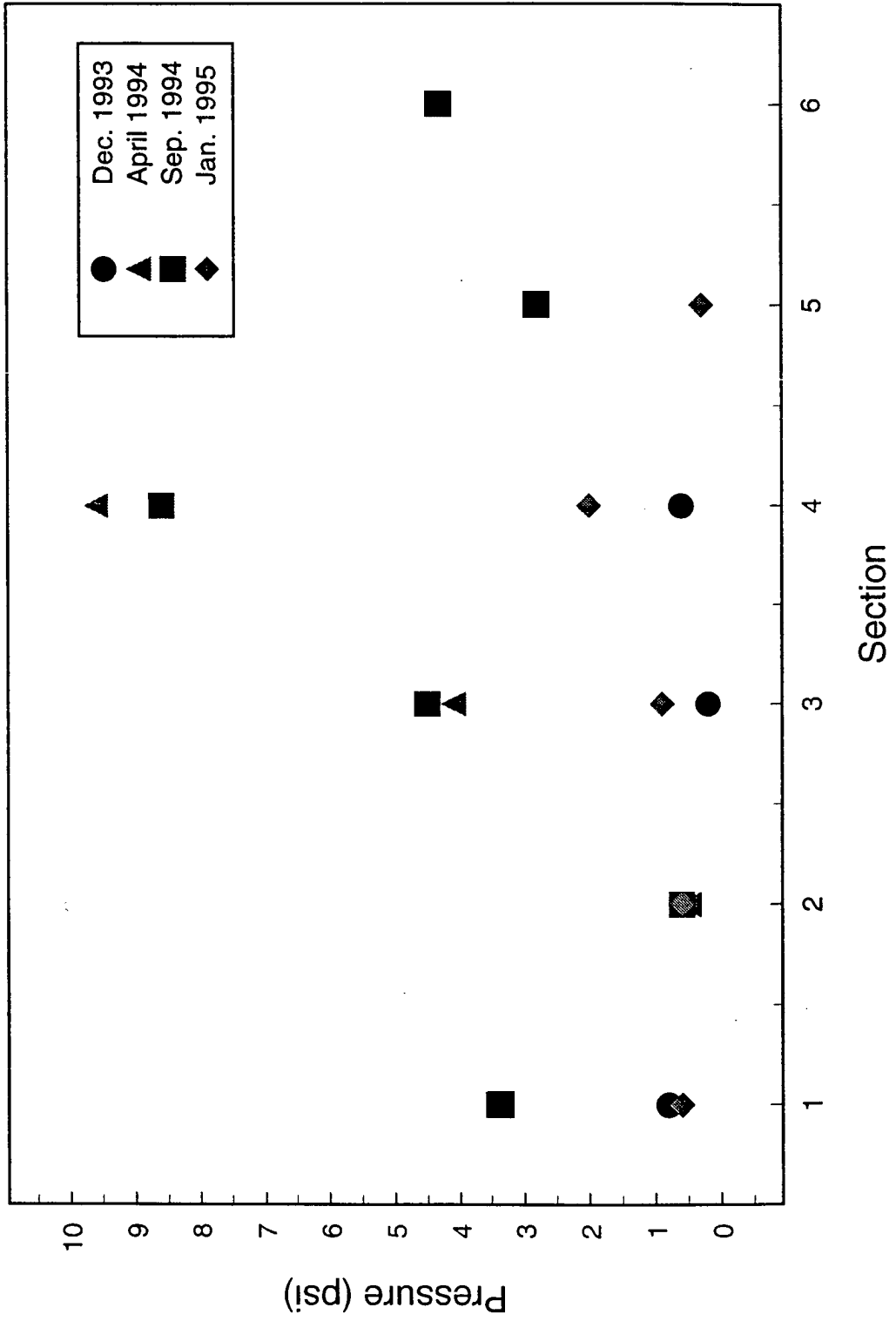


Figure 5.10 Subgrade Pressures Versus Section

Table 5.5 Strain Gauge Response for FWD

Month Tested	Section	Load (lb)	Pavement Temperature (°F)	Strain Gauges Monitored	Strain (E-6)	
December	1	14280	32	DYN01	27	
		14840	32	HBM01	36	
		14840	39	HBM02	-60	
	2	15392	33	DYN01	27	
		15392	37	DYN02	-22	
		14864	33	HBM01	24	
		14864	37	HBM02	-27	
	3	15064	32	DYN01	15	
		15064	34	DYN02	-19	
		15912	32	HBM01	10	
		15912	34	HBM02	-17	
	4	15432	31	HBM01	20	
		15432	32	HBM02	-150	
	April	2	15300	66	DYN01	23
			15300	71	DYN02	-22
			15344	66	HBM01	11
3		15100	67	HBM01	250	
		15100	75	HBM02	-650	
4		15208	71	DYN01	110	
		15550	71	HBM01	66	
		15550	84	HBM02	-45	
September		1	16596	62	HBM01	40
	16596		63	HBM02	-35	
	2	16416	63	DYN01	20	
		16416	64	DYN02	-10	
		16500	63	HBM01	14	
		16500	64	HBM02	-46	
	3	16080	66	HBM01	170	
		16080	68	HBM02	-10	

Table 5.5 Strain Gauge Response for FWD (continued)

Month Tested	Section	Load (lb)	Pavement Temperature (°F)	Strain Gauges Monitored	Strain (E-6)	
September (continued)	4	15992	69	DYN01	95	
		15872	69	HBM01	82	
		15872	69	HBM01	-70	
	5	15832	70	DYN01	110	
		15832	73	DYN02	-15	
		15794	70	HBM01	36	
		15794	73	HBM02	-60	
	6	15864	70	DYN01	35	
		15864	73	DYN02	-15	
		15752	70	HBM01	30	
	January	1	17161	35	HBM01	22
		2	17463	37	DYN01	13
17463			35	DYN02	-12	
3		17701	37	HBM01	84	
4		18321	37	DYN01	6	
	18241	37	HBM01	16		
	18241	38	HBM02	-21		
5	17430	37	DYN01	34		

for Section 1, Dynatest and HBM strain gauges measured tensile strains at the bottom of the asphalt concrete of 27 and 36 micro-strain, respectively. The HBM gauge read a compressive strain of -60 micro-strain at the top of the asphalt concrete. For September, HBM gauges read 40 and -35 micro-strain. During January, a reading of 22 micro-strain was recorded for the bottom HBM gauge. Typical responses for Dynatest and HBM gauges are shown in Figure 5.11.

For Section 2, tests conducted in December and January, the bottom Dynatest gauge recorded strains of 27 and 13 micro-strain, respectively. The HBM gauge recorded 24 micro-strain for the December test. The top gauges for these tests read -22 and -12 micro-strain for the Dynatest and -27 for the HBM in December. In April and September, the readings for the Dynatest gauge were 23 and 20 micro-strain, respectively, for the bottom gauges and -22 and -10 micro-strain for the top gauges. In April, the bottom HBM gauge recorded a response of 11 micro-strain for the FWD test. In September, the responses for the HBM gauges were 14 and -46 micro-strain for top and bottom gauges. The top HBM gauge recorded strains of -27 micro-strain in December and -46 micro-strain in September.

Testing of Section 3 in December yielded the most complete set of strain data. Dynatest and HBM measurements in the top layer of the asphalt concrete pavement were -19 and -17 micro-strain. Values of 15 and 10 micro-strain were measured at the bottom of the asphalt concrete. Dynatest strain response is pictured in Figure 5.12. The response of the HBM gauges was similar to the Dynatest gauges. Top gauge response was always larger in magnitude than the bottom gauge response. The top gauges were in compression, whereas, the bottom gauges were in tension.

In Section 4, the bottom Dynatest gauge recorded a response of 110 and 95 micro-strain in

SECTION 1 HBM RESPONSE  
Falling Weight Deflectometer December Test

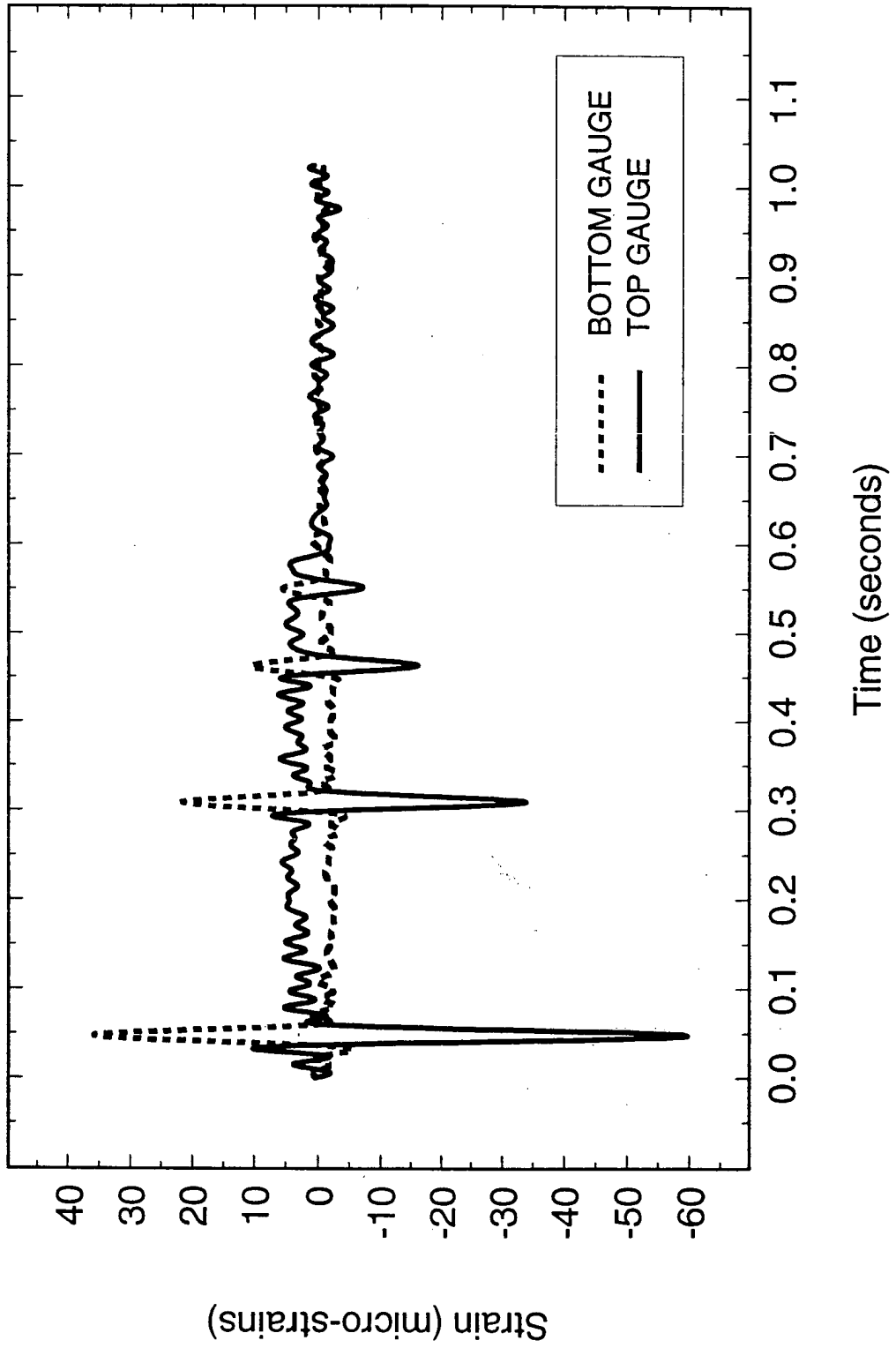


Figure 5.11 HBM Response to FWD Testing

### SECTION 3 DYNATEST RESPONSE

Falling Weight Deflectometer December Test

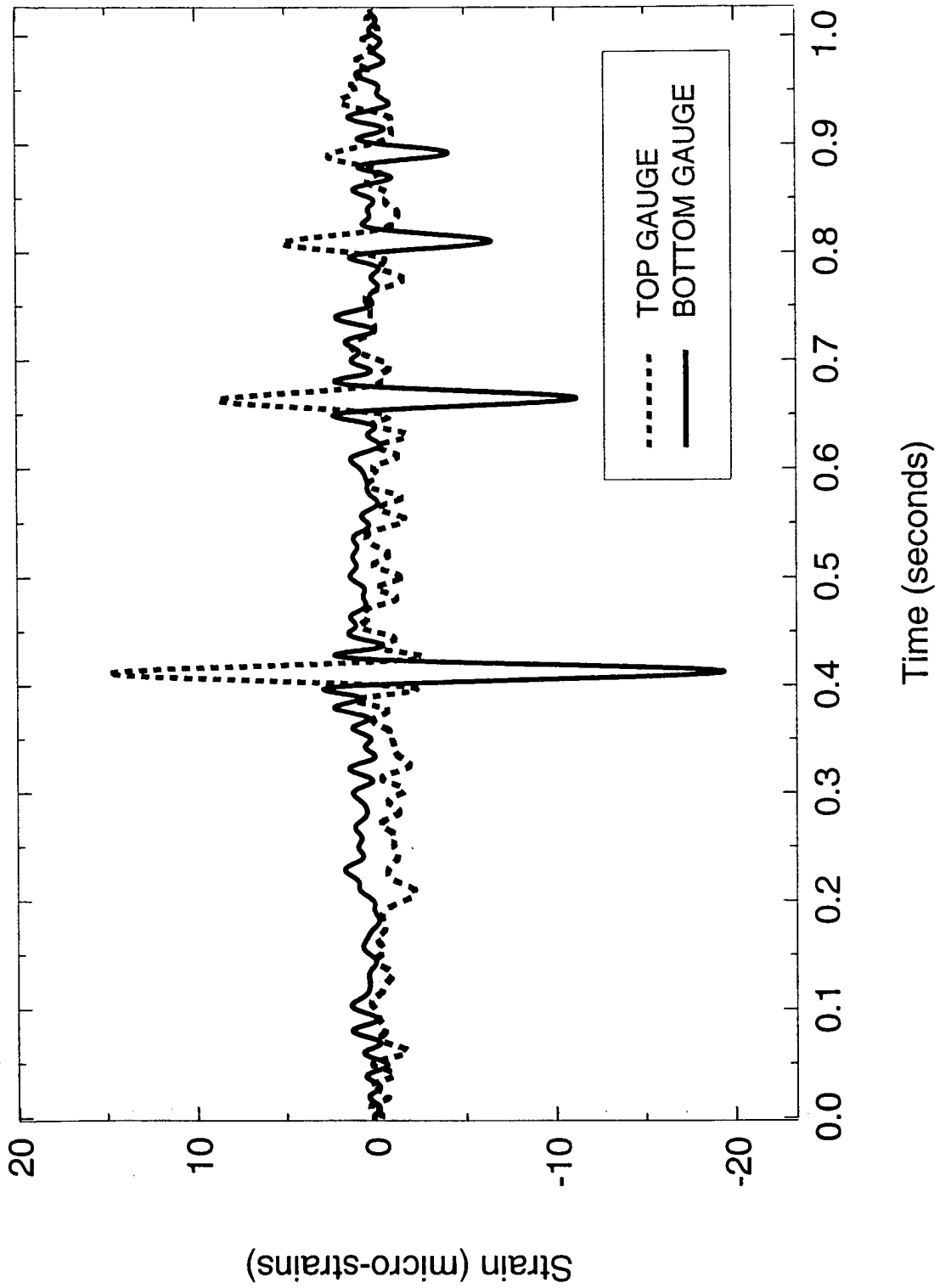


Figure 5.12 Dynatest Response to FWD Testing

April and September, respectively. For the January test, 6 micro-strain was measured by the bottom gauge. These readings support the previous observation that larger responses are expected during the warmer months. Both HBM gauges responded during the tests. The bottom gauge gave responses of 20 and 16 micro-strain for December and January, and 66 and 82 micro-strain for April and September. Readings of -45 and -70 micro-strain for April and September were recorded for the top gauge, while the readings for December and January were -150 and -21, respectively.

Strains were measured for two FWD tests on Section 5. Strains measured at the top of the pavement were -15 micro-strain for the Dynatest gauge and -60 micro-strain for the HBM gauge. Values of 110 micro-strain by the Dynatest gauge and 36 micro-strain by the HBM gauge were measured at the pavement lower side. Testing in January yielded only strain from the bottom Dynatest gauge of 34 micro-strain.

In Section 6 for September, both Dynatest gauges responded to the FWD test giving readings of 35 micro-strain for the bottom gauge and -15 micro-strain for the top. The bottom HBM gauge measured 30 micro-strain.

Data taken from the December test show compressive and tensile strains measured at Section 1 to be larger than the strains measured at other sections. This supports conclusions drawn from deflection and pressure data that during the December test Section 1 was more flexible. Of note also is the magnitude of the compressive strain at the top of the asphalt concrete layer. Both the Dynatest and HBM gauges show the compressive strain to be larger than the tensile strain found at the bottom of the asphalt concrete. This can be attributed to the proximity of the load and the difference in temperature between the top and bottom of the pavement.

The strains of Section 4 are significantly larger than those in Section 2 for both the Dynatest

and HBM gauges. With the soil moisture and temperature being relatively the same, this difference must be attributed to the different base materials.

During several tests, a few gauges responded the same in tension or compression for the same drop. To examine this phenomenon, during the September FWD a test was conducted on Section 6 where the location of the drop was varied. The load was dropped directly over the Dynatest gauge and the responses were recorded. Then a load was dropped about 3 inches from the center of the gauge and this response was also recorded. During the analysis of the two drops, it was noted that for the first drop both the top and bottom gauges responded in tension, but during the second drop the gauges responded with the top in compression and the bottom in tension. Thus, it was concluded that the proximity of the FWD load indicated a loose anchoring on formation of a small crack in the asphalt concrete.

#### **5.4 SUMMARY**

Results from data analysis conclude that the cement treated base is the stiffer of the five bases with the asphalt concrete treated base being the most flexible at high temperature. Analysis of the "304 type bases" (i.e., NJ, IA, 304) displayed varying results. Each base appeared best under specific conditions. On the average, the NJ base appeared to be the stiffest.

Agreement between the geophone and LVDT results show that both measurement techniques are consistent and may be interchanged for particular applications.

It appears after cyclic loading there is damage. At warm temperatures the aggregate may rearrange and damage the strain gauges. The Dynatest performed better than HBM with fewer casualties. The gauges installed in the top and bottom of pavement are not the same because of temperature difference and because friction between base and asphalt concrete affect the strain field.



## CHAPTER 6

### MODELING OF FLEXIBLE PAVEMENTS

#### 6.1 INTRODUCTION

The ability to predict the response of flexible pavements, base, and subgrade soils is important for designing, maintaining, and rehabilitating pavements. A useable model of flexible pavement enables the engineer to better design the thickness and performance requirements of materials in the pavement, base, and subgrade layers. Also important is the variation of pavement response under conditions of heavy loads and seasonal weather changes, particularly increased soil moisture. Flexible pavement response can be determined using extensive instrumentation, but the cost, time requirements, and data interpretation makes the use of non-destructive testing (NDT) in conjunction with finite element backcalculation a very attractive, cost efficient alternative.

In this study of six sections of flexible pavements, three were extensively instrumented and the results were analyzed. Flexible pavement deflections were modeled with the OU-PAVE program. Calculations were performed with the published parameters. This calculation provides insight into the role of pavement design features with the modulus of subgrade soils and also on the general characteristics of asphalt concrete response at the test sites.

#### 6.2 MATERIAL PROPERTIES

There are a number of studies that indicate that the linear elastic model does not adequately characterize the pavement system. Linear response, while providing a useful solution, does not correspond to field properties because of the importance of the stress path, moisture content of the

base and subgrade, soil density, and temperature of flexible pavement. The dynamic application of load and repeated loadings must also be accounted for in the analysis.

### **6.2.1 Asphalt Concrete Pavement**

The Asphalt Institute equations (10) are currently the most widely used for determining modulus as a function of temperature. These were used to determine input for the OU-PAVE program. The equations are based on standard tests under sinusoidal loadings at 1, 4, and 16 Hz for temperatures of 4, 21, and 38°C. Age and seasonal variations are also important.

### **6.2.2 Base**

Bases were treated as a linear elastic material. Elastic constants were obtained from a literature review. These values were maintained at initial magnitudes except for the asphalt treated base where the value of modulus was modified with temperature change. For Section 3, all calculations were completed with an elastic modulus of 35,000 psi and Poisson's ratio of 0.25. The elastic modulus of 25,000 and Poisson's ratio of 0.25 was used for Section 5.

### **6.2.3 Subgrade**

The fine-grained soils were modeled with an arithmetic model shown in Figure 6.1. This model was developed after extensive triaxial testing by Thompson and Robnett (11). Additional testing, including FWD, has indicated that this model is appropriate for OU-PAVE computations (12). The two slopes used in the analysis was  $K_1 = -1100$  and  $K_2 = -178$ . Since the moisture remained almost the same in all seasons, the same parameters were used in all calculations.

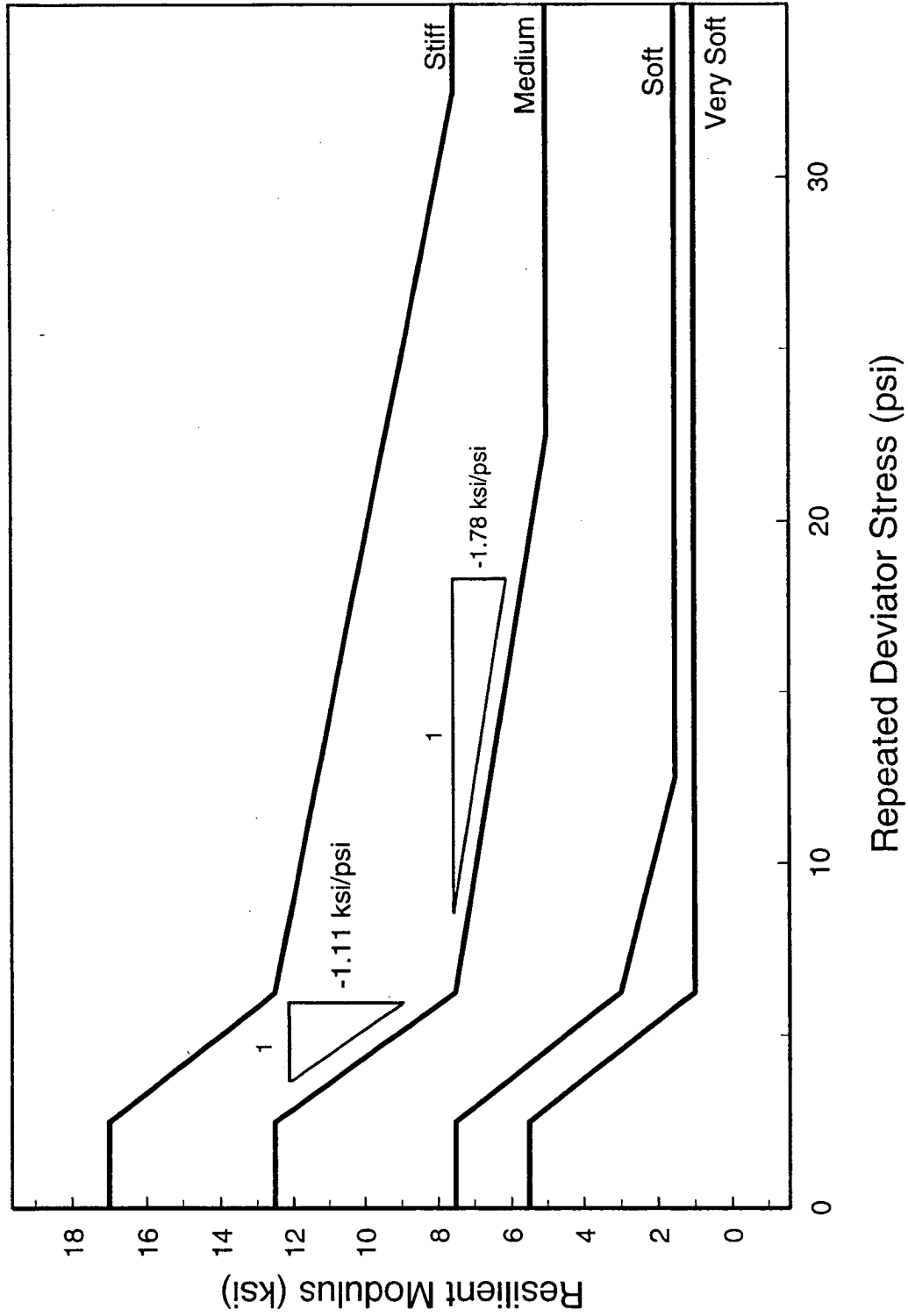


Figure 6.1 ILLI-PAVE Subgrade Materials Models for Stiff, Medium Stiff, Soft and Very Soft Soils from "19"

### **6.3 MODELING FLEXIBLE PAVEMENTS WITH OU-PAVE**

The responses of the three flexible pavement test sites were modeled with OU-PAVE. Data was collected on available sections so that seasonal variations could be examined with the OU-PAVE model. Data was collected in April for Section 3; in September for Sections 1, 3, and 5; and in January for Sections 1, 3, and 5. Modeling was done for one loading for each season at each site. Each pavement had three layers: asphalt concrete, base, and subgrade. The thicknesses of the top layers and classification of pavement at each site are given in Chapter 2. The base characteristics are given in Table 2.1. Each site was simulated with an axisymmetric model. The mesh was essentially the same for all sites with only details of the mesh varied to correspond to a particular site.

The symmetry of the problem allowed the solution to be specified in terms of plane a radial section. An axisymmetric mesh with 400 four-node rectangular elements was used to represent each section. The nodes at the inner and outer vertical boundaries were constrained to move vertically, the lower boundary was completely fixed, and all other nodes were free to move in both directions. The mesh had a 150 inch radius from the load to the outer edge; the mesh was more than 300 inches deep.

### **6.4 APRIL EVALUATION OF FEM AND FWD DATA**

In the April results for Section 3 (NJ Experimental Base), FEM calculations matched the large deflection recorded at the center of the deflection basin, as shown in Figure 6.2. The measured deflection basin shows almost exact agreement when compared to FEM. This confirms other recorded data where contact pressures of 4.1 and 6.5 psi were measured at the boundaries of

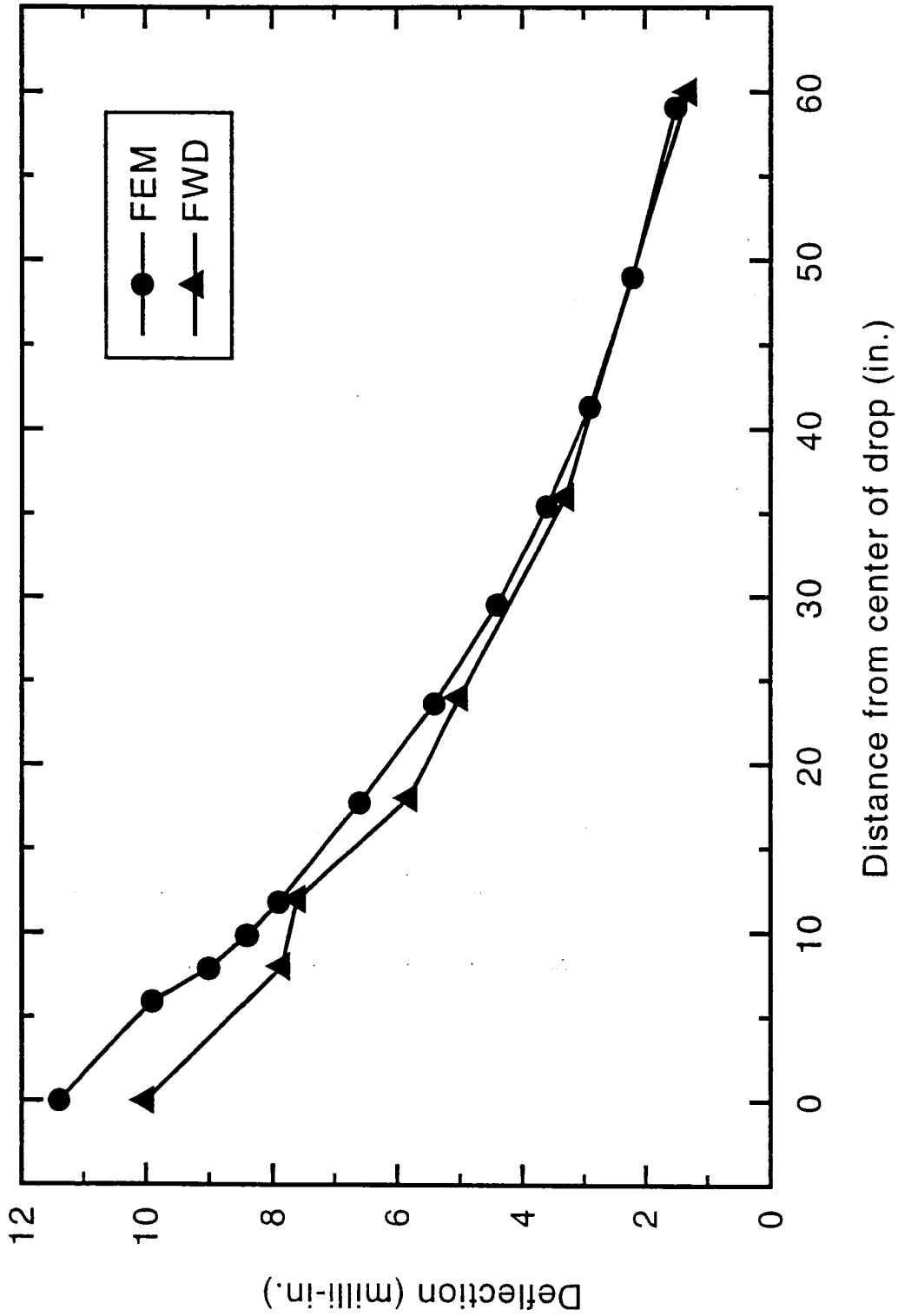


Figure 6.2: Comparison of FWD Deflections of Section 3 for April Test

base/subgrade and pavement/base, respectively. These values were 5 and 6 times the values measured in January.

## **6.5 SEPTEMBER EVALUATION OF FEM AND FWD DATA**

In the September results for Section 1 (Asphalt Treated Base), FEM calculation closely resembled the field data as shown in Figure 6.3. However, the magnitude of FEM calculations was approximately 1 milli-inch less. Results for Section 3 (NJ Experimental Base) are compared in Figure 6.4. September field deflections were considerably less than the April measurements, while FEM results, based on input data for April, exhibited the same deflection profile. The September results for Section 5 (crushed 304) showed a localized basin, whereas, the FEM model predicted a deep shallow basin as shown in Figure 6.5. Maximum deflections calculated by the FEM were 14.0, 8.2, and 9.2 milli-inches for Sections 1, 3, and 5, respectively. Maximum measured geophone deflections were 12.2, 6.5, and 11.7 milli-inches for Sections 1, 3, and 5, respectively.

## **6.6 JANUARY EVALUATION OF FEM AND FWD DATA**

The profiles for Section 1 (ATB), Section 3 (NJ) and Section 5 (crushed 304) for January are shown in Figures 6.6, 6.7, and 6.8, respectively. Profiles match the FEM calculations well. However, the discrepancies exist between maximum deflections that were measured in comparison to calculated values. Maximum deflections measured for Sections 1, 3, and 5 are 6.3, 4.1, and 5.4 milli-inches, whereas, the FEM calculates maximum deflections of 6.4, 6.1, and 6.4 milli-inches.

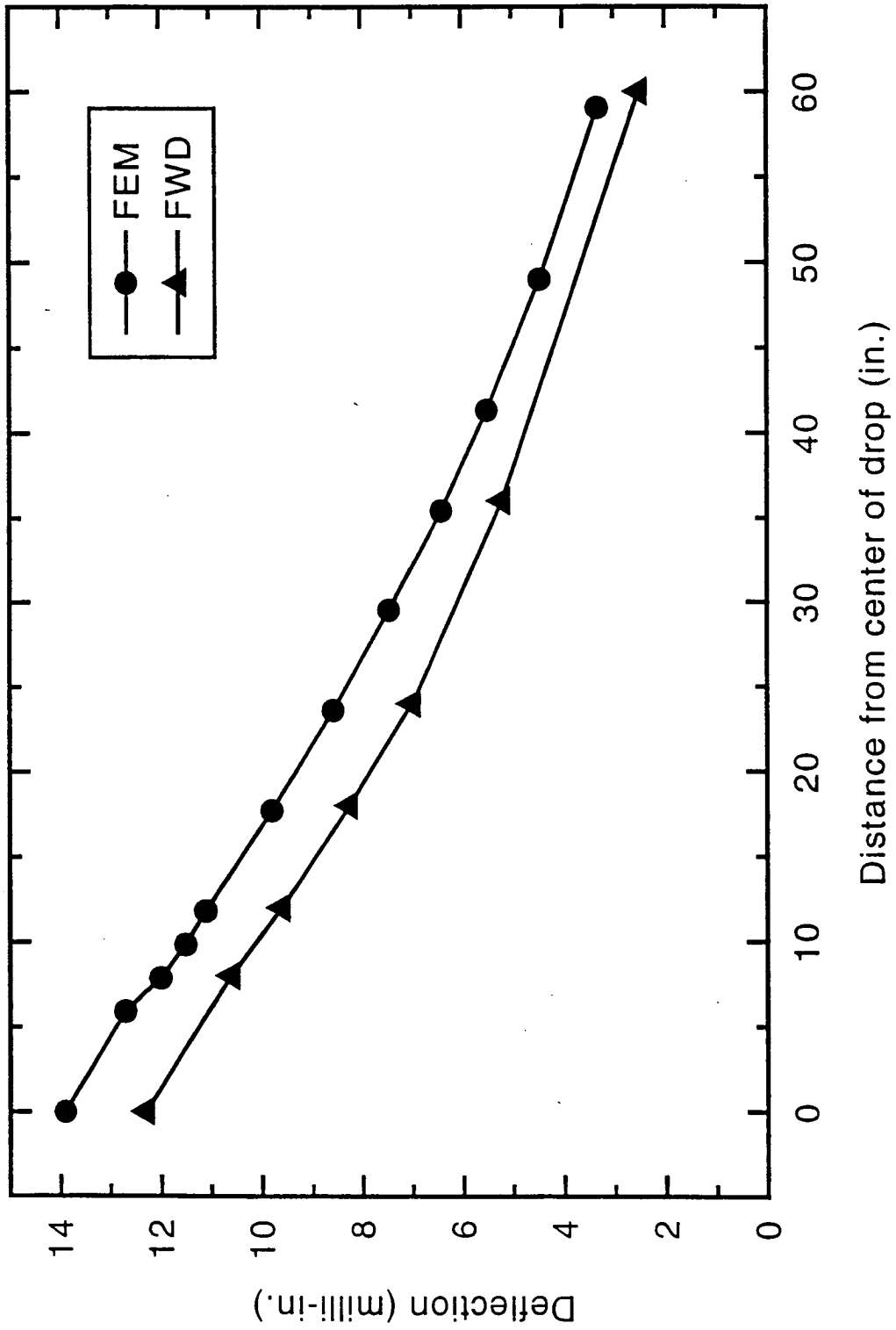


Figure 6.3: Comparison of FWD Deflections of Section 1 for September Test

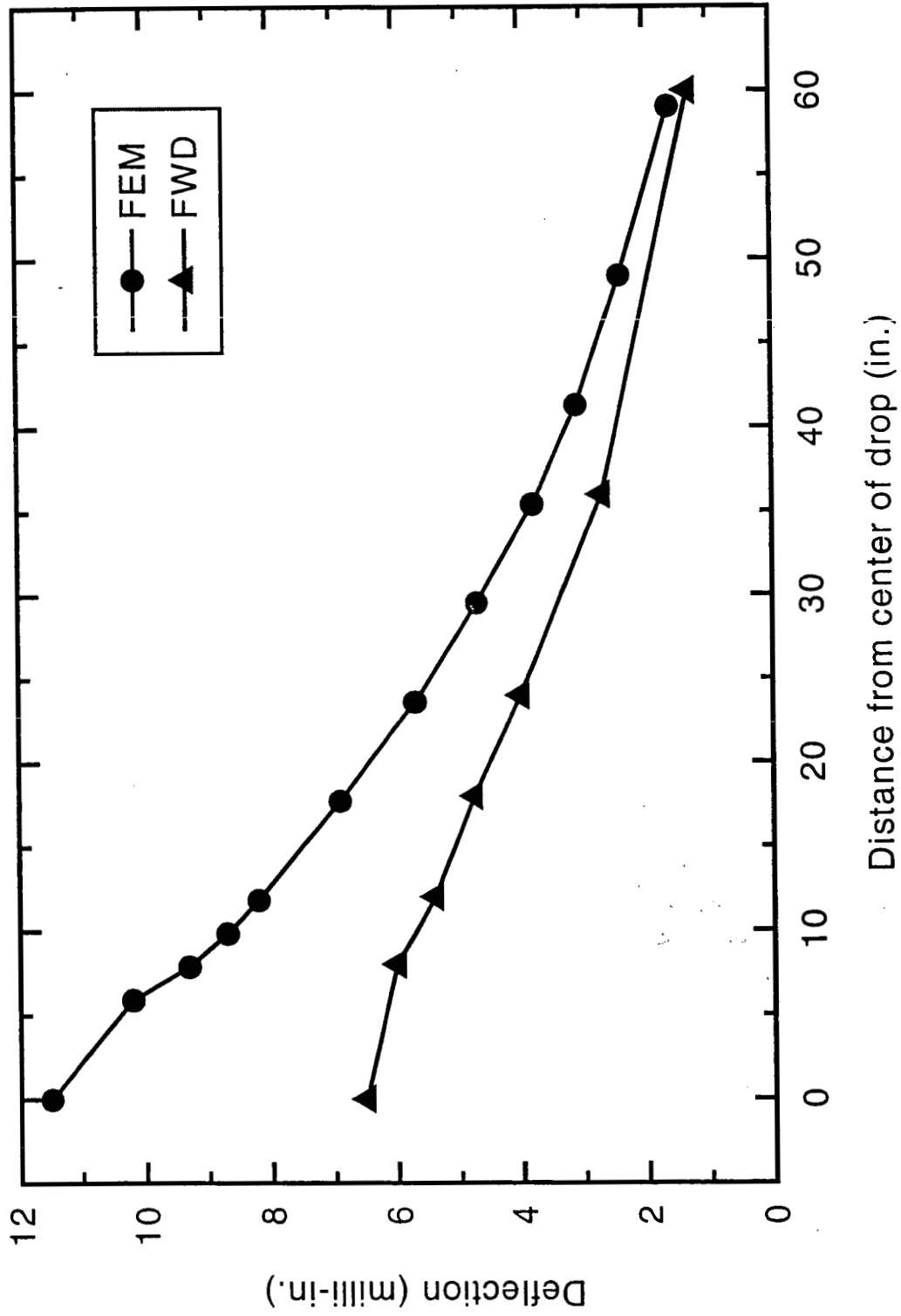


Figure 6.4: Comparison of FWD Deflections of Section 3 for September Test

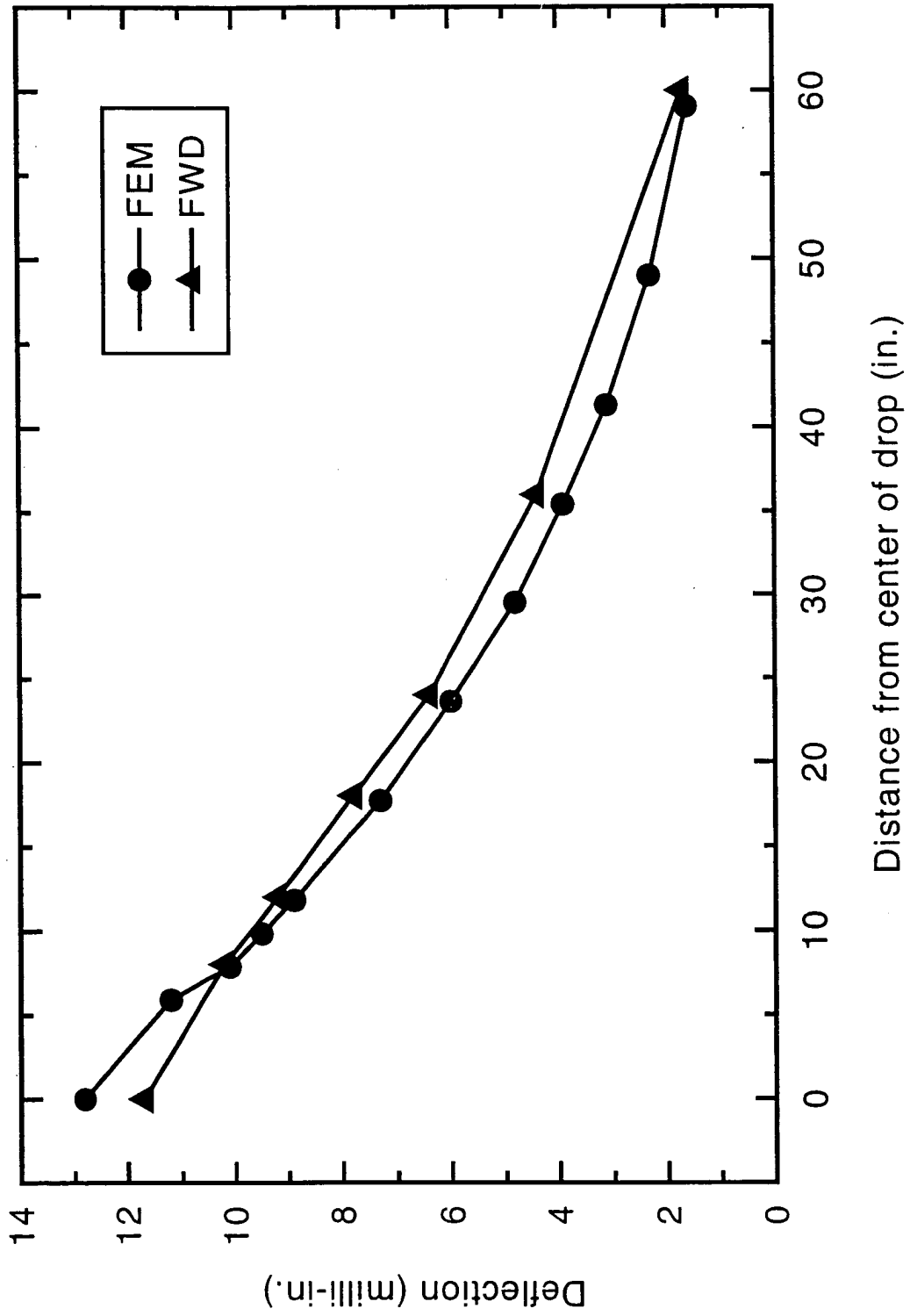


Figure 6.5: Comparison of FWD Deflections of Section 5 for September Test

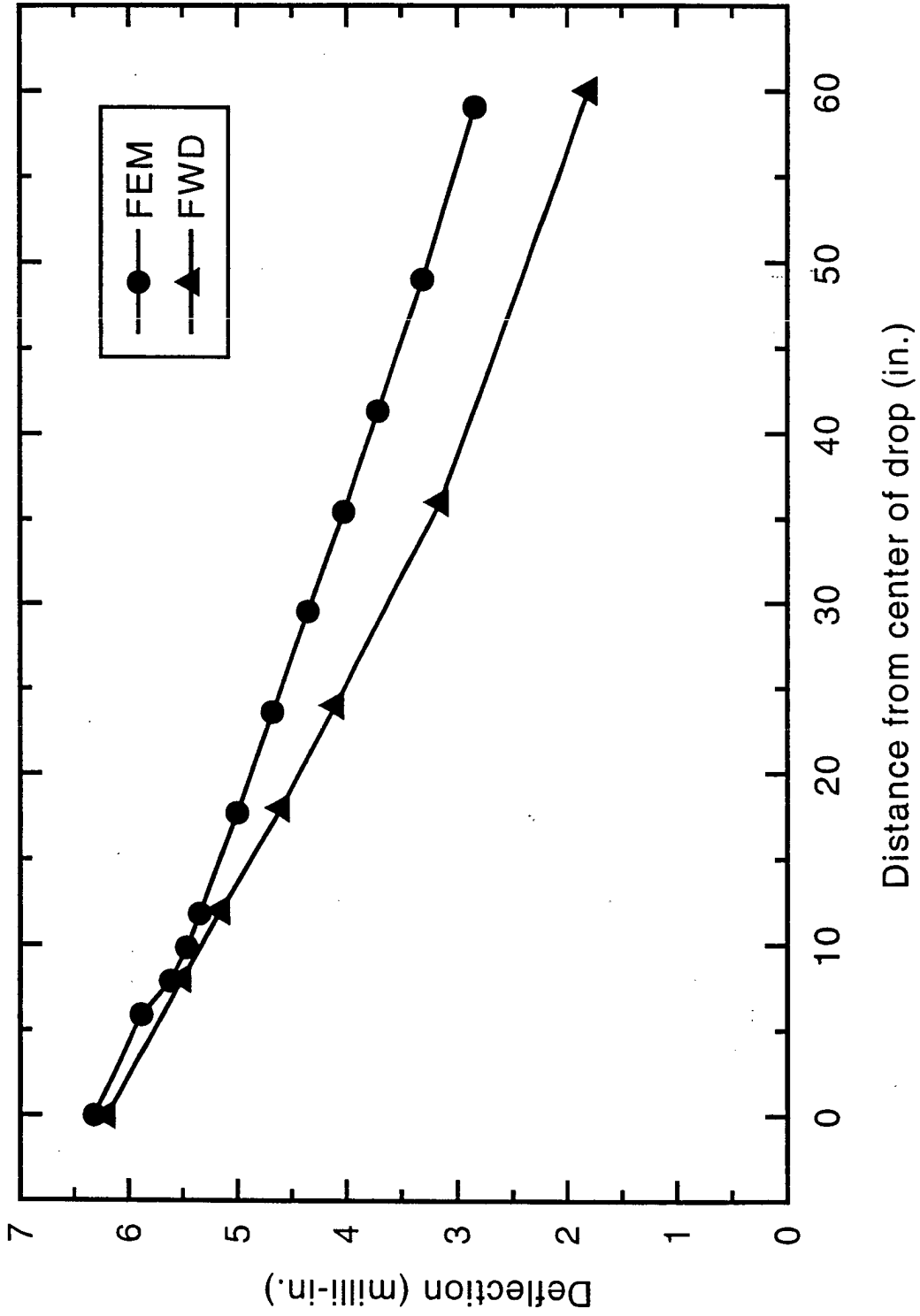


Figure 6.6: Comparison of FWD Deflections of Section 1 for January Test

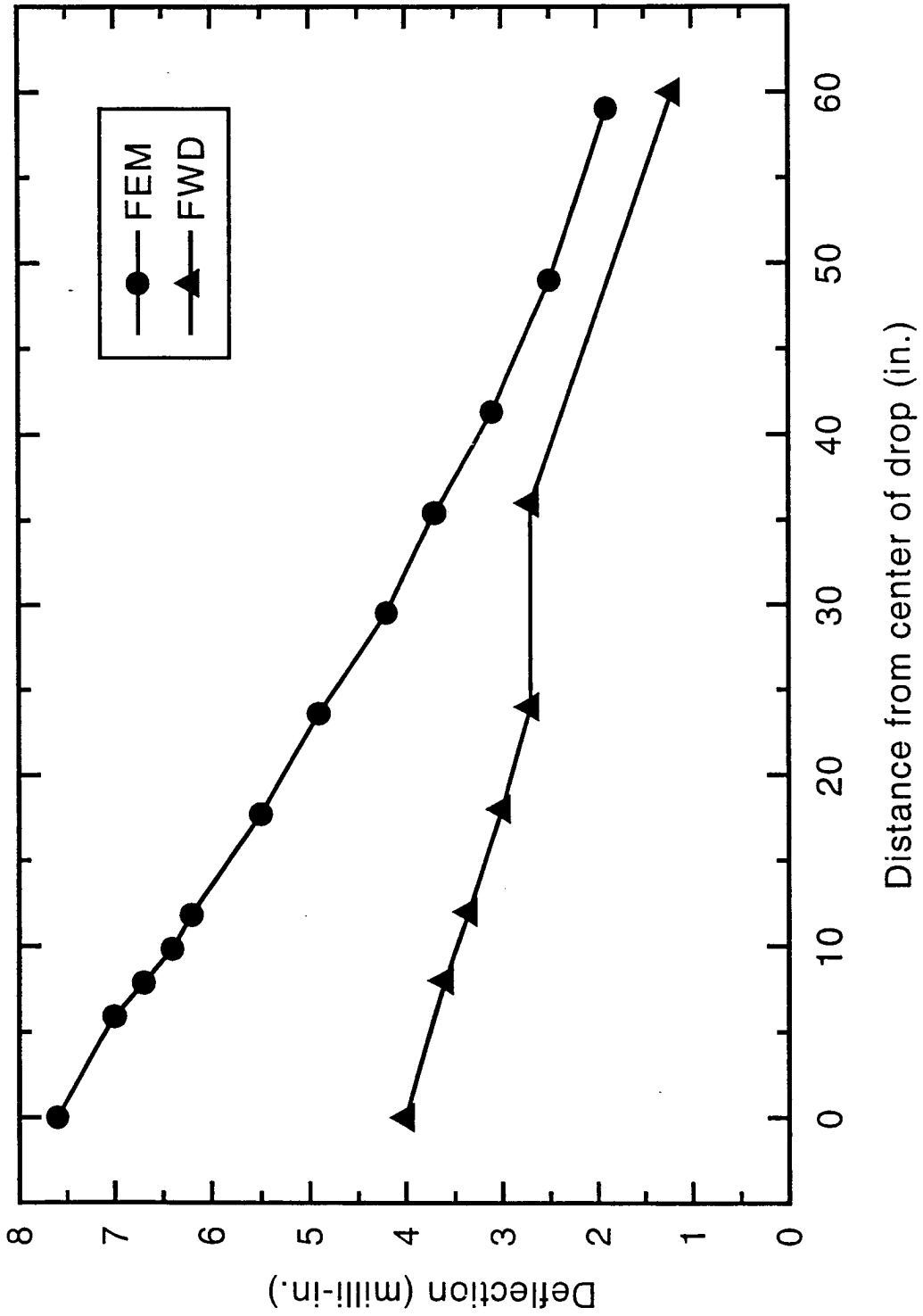


Figure 6.7: Comparison of FWD Deflections of Section 3 for January Test

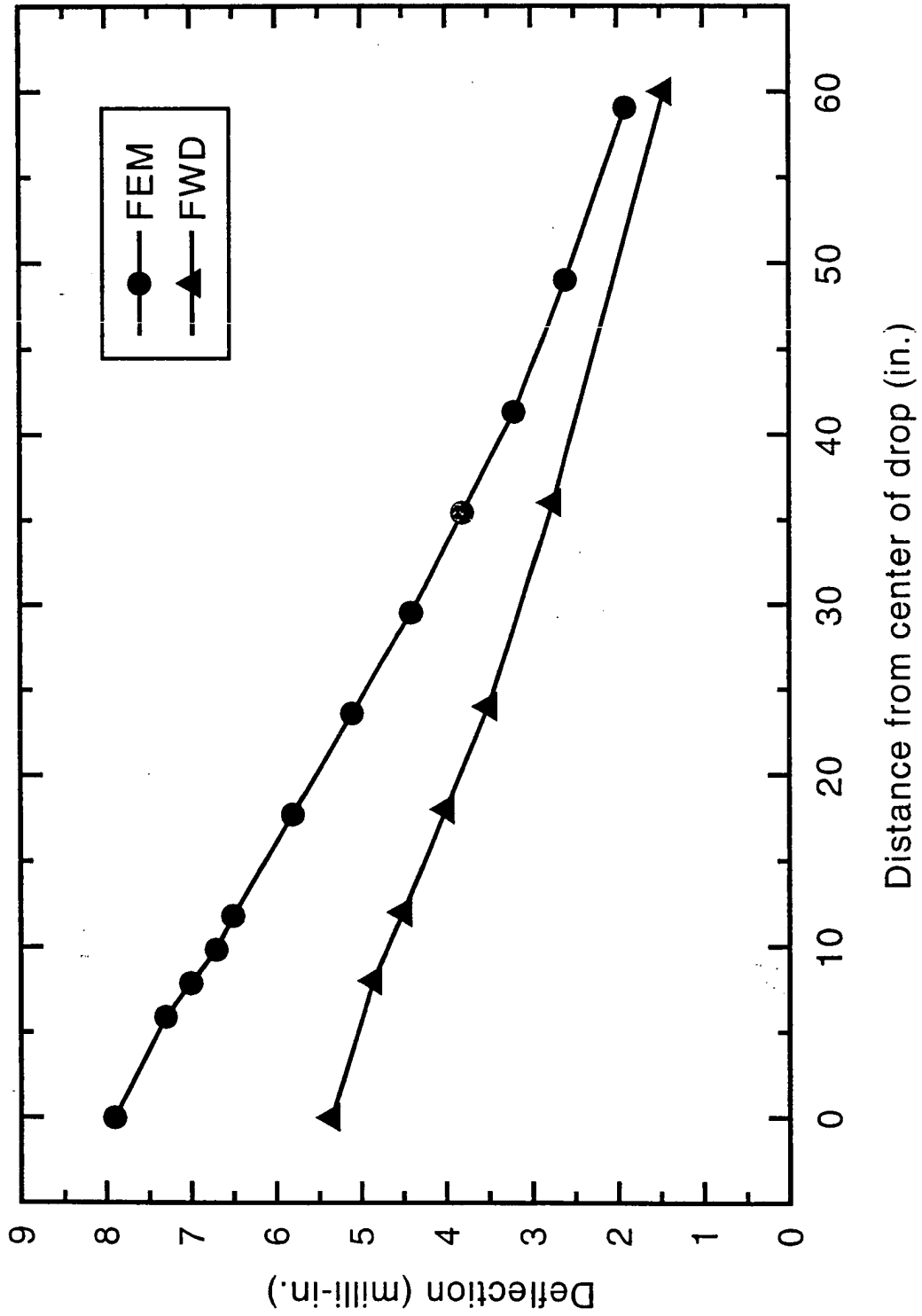


Figure 6.8: Comparison of FWD Deflections of Section 5 for January Test

## **6.7 DISCUSSION OF RESULTS**

The FEM calculates a reasonable deflection profile for FWD testing using standard input parameters. No attempt was made to alter the parameters to make the data match. The greatest discrepancies occur for winter and spring where deflections predicted for winter are much higher than those measured and the deflections predicted for spring are lower than calculated. The finite element predicted results could be in good agreement with field results if the true material properties were determined from laboratory testing to be incorporated into the finite element formulation.



## CHAPTER 7

### CONCLUSIONS AND RECOMMENDATIONS

#### 7.1 CONCLUSIONS

This project comprised installation, sensor performance, and comparison of six types of bases for an asphalt concrete pavement. In addition, flexible pavement deflections were modeled with the OU-PAVE program and compared to field results from FWD.

#### 7.2 SUMMARY

##### 7.2.1 Sensor Installation

Asphalt concrete sieved through wire mesh provided an adequate barrier against damage to the gauges from larger aggregate and temperature. Positioning the instrumentation just ahead of the paver guaranteed that the asphalt concrete temperature would be high enough for complete bonding of sensors to pavement. Prohibiting the use of vibratory rollers over the sensors prevented damage from occurring during compaction. The installation procedures contributed to 117 of the 120 sensors being installed successfully. The installation of sensors was successful; however, only 60% of the sensors could be used in recording data.

##### 7.2.2 Sensor Performance

The performance of the installed sensors was of expected quality.

- Thermocouples and soil moisture probes provided accurate data on existing environmental conditions under the pavement.
- Deflections measured by accelerometers and LVDTs paralleled the readings recorded by the

FWD geophones. LVDTs can be used to obtain base and subgrade movements. Anchoring the displacement rods at a depth of 10 feet proved satisfactory.

- Strain Gauge Pressure Cells were successful in measuring the magnitude of pressures at the pavement/base and base/subgrade interfaces under NDT.
- Dynatest and HBM strain gauges were well suited for measuring strain in the asphalt concrete. However, installation procedures must be carefully adhered to. Both gauges gave consistent measurements when compared to each other.

The Dynatest strain gauges are the only ones that have been used successfully. The HBM gauges were vulnerable at the wire and sensor connection. The wire would burn at this location during installation. However, the longevity is questionable. In future projects, installation of LVDTs for measuring displacement should take place during construction. After completion of construction when drilling takes place, as the drill core is removed, in many cases, the material will cave in, particularly if unbonded base material is used, and this creates a void under the pavement. During the Falling Weight Deflectometer (FWD) test, displacement measured with the accelerometer and LVDT correlated very well. At low frequency, obviously, the accelerometer will not be as accurate as the LVDT.

### **7.2.3 Pavement and Base Performance**

Of the six types of bases used under the asphalt concrete in Route 33 and evaluated for influence on the deflection of pavement, deflection measurements for the asphalt treated base fluctuated the most due to a change in temperature. It is obvious that all other bases are not a function of temperature. Under the same load condition, the deflection with cement treated base was lowest of all bases. In the case of the unbound material, the bases that contained large size stone

resulted in less deflection.

However, before making final recommendations on the relative performance of each base, it must be determined how these bases behave after the pavement has experienced long term traffic loading. Particularly, the structural integrity of the asphalt and cement treated bases will be effected by the cyclic loading of traffic.

The moisture in the subgrade stayed fairly constant in this study because the asphalt was new; however, observations should be made as the asphalt ages and water penetrates to the bases. Hence, the effectiveness of these bases on removal of water should be investigated. Even though the cement treated base reduced displacement, how this will effect the long term performance should be evaluated by conducting a distress survey. This is a very important point because if the base is rigid the asphalt will experience a different stress path condition than if the base is flexible.

Pressure readings were consistent with deflection measurements. Larger values were recorded during April and September. FWD testing of ATB in September yielded a smaller pressure at the pavement/base interface than for the other sections. The highest pressures of the PCTB were recorded at the pavement/base interface during September and April. Data taken from the December test show compressive and tensile strains measured in ATB larger than the strains in the other sections. This supports the conclusions drawn from deflection and pressure data that even during the colder months, ATB was the most flexible.

The attempt that was made in this investigation to verify the usefulness of OU-PAVE showed the value of a finite element calculation. This program can be utilized in back calculation where material constants are determined from FWD loading. With an axiasymmetric mesh configuration FEM calculates an accurate maximum deflection and a reasonable deflection profile for FWD testing.

### 7.3 RECOMMENDATIONS

Based on this result in modeling, the pavement system can be used with high confidence. The results of this investigation concerning future instrumentation, data collection, and data analysis of flexible pavements should be implemented according to the following recommendations:

- The installation procedure for sensors in flexible pavement was successful and should be followed by future investigators.
- The single anchor LVDT is reliable for measuring FWD induced deflections of the flexible pavement with respect to the anchor.
- Pavement design procedures should continue to account for high contact pressures on the subgrade that occur during the warmer months.
- A nonlinear formulation for asphalt concrete response to loading should be formulated.
- The long term performance of bases should be investigated: How permeability of bases changes with respect to time and failure mode or distress of asphalt concrete changes with respect to time and type of base.

## REFERENCES

1. Bonaquest, R., Surdahl, R., Mogawer, W. *Effect of Tire Pressure on Flexible Pavement Response and Performance*, Transportation Research Record 1227 - Rigid and Flexible Pavement Design and Analysis, (1989), p. 97-106.
2. Sebaaly, P.E. Tabatabaeo, N., Scullion, T. *Comparison of Backcalculated Moduli from Falling Weight Deflectometers and Truck Loading*, Transportation Research Record 1377 - Nondestructive Deflection Testing and Backcalculation for Pavements, (1992) p. 88-98.
3. Tabatabaee, Nader and Sebaaly, Peter. *State of the Art Pavement Instrumentation*, Transportation Research Record 1260-Measurement of Pavement Surface Conditions, (1990), p. 246-255.
4. Brown, S.F. *State of the Art Report on Field Instrumentation for Pavement*, Transportation Research Record 640, Transportation Research Board, Washington, D.C. (1977), p. 13-27.
5. Ullitz, Per and Busch, Christian. *Laboratory Testing of a Full-Scale Pavement: The Danish Road Testing Machine*, Transportation Research Record 715, Transportation Research Board, Washington, D.C. (1979), p. 52-62.
6. Nazarian, Sohail and Chai, Y.E. *Comparison of Theoretical and In-Situ Behaviors of a Flexible Pavement Section*, Transportation Research Record 1377-Pavement Design, Management and Performance, (1992), p. 172-182.
7. Kim, Y.R., Khosla, N.P., Satish, S., Scullion, T. *Validation of Moduli Backcalculation Procedure Using Multi-Depth Deflectometers Installed in Various Flexible Pavement Structures*, Transportation Research Record 1377-Pavement Design, Management and Performance, (1992), p. 128-142.
8. Edwards, William F., Green, Roger L., Gilfert, James. *Implementation of a Dynamic Deflection System for Rigid and Flexible Pavements in Ohio*, Report FHWA/OH-89/020, The Ohio Department of Transportation, Columbus, Ohio (1989).
9. Kelly, Henry Francis, Jr. *Development of Mechanistic Flexible Pavement Design Concepts for the Heavy Weight F-15 Aircraft*, Ph.D. Thesis, University of Illinois, Urbana-Champaign, (1986).
10. The Asphalt Institute. *Research and Development of the Asphalt Institute Thickness Design Manual (MS-1), Ninth Edition*, Research Report No. 82-2, Maryland.



11. Thompson, M.R. and Robnett, Q.L. *Final Report, Resilient Properties of Subgrade Soils*, Civil Engineering Studies, Series No. 160, University of Illinois, Urbana-Champaign, (1976).
12. Sargand, S.M. and Hazen, G.A. *Evaluation of Resilient Modulus by Back-Calculation Technique*, Final Report No. FHWA/OH-91/005, (1991).

